Applications of Mathematics

Vladimír Janovský; Viktor Seige

A global analysis of Newton iterations for determining turning points

Applications of Mathematics, Vol. 38 (1993), No. 4-5, 323–360

Persistent URL: http://dml.cz/dmlcz/104559

38 (1993) APPLICATIONS OF MATHEMATICS No. 4–5, 323–360

A GLOBAL ANALYSIS OF NEWTON ITERATIONS FOR DETERMINING TURNING POINTS

VLADIMÍR JANOVSKÝ and VIKTOR SEIGE, Praha

Summary. The global convergence of a direct method for determining turning (limit) points of a parameter-dependent mapping is analysed. It is assumed that the relevant extended system has a singular root for a special parameter value. The singular root is classified as a *bifurcation singularity* (i.e., as a *degenerate* turning point). Then, the Theory for Imperfect Bifurcation offers a particular scenario for the split of the singular root into a finite number of regular roots (turning points) due to a given parameter imperfection. The relationship between the scenario and the actual performance of Newton method is studied. Both theoretical and experimental arguments are presented in order to question the claim that a particular bifurcation singularity *organizes* the Newton method assuming small parameter perturbations.

Keywords: detection of turning points, Newton method, Newton flow, basins of attraction, qualitative analysis, normal forms of the flow

AMS classification: 65H20, 58C15

1. MOTIVATION

Let $F\colon \mathbf{R}^N \times \mathbf{R}^1 \times \mathbf{R}^k \to \mathbf{R}^N$, $F = F(u, \lambda, \alpha)$, be a smooth mapping. In the bifurcation context, see e.g. [2], the equation $F(u, \lambda, \alpha) = 0$ defines implicitly the dependence $\lambda \mapsto u$ of a *state variable* u on a (scalar) *control parameter* λ while an *imperfection parameter* $\alpha \in \mathbf{R}^k$ is fixed.

A point $(u^*, \lambda^*, \alpha^*) \in \mathbf{R}^N \times \mathbf{R}^1 \times \mathbf{R}^k$ is a *singular point* provided that

$$F(u^*, \lambda^*, \alpha^*) = 0, \quad \dim \operatorname{Ker} F_u(u^*, \lambda^*, \alpha^*) = m, \quad m \geqslant 1.$$

The dimension m is called *corank* of the singular point. Singular points can be classified in accordance with qualitative properties of the *(perfect) bifurcation diagram*

$$\mathscr{S} = \{(u, \lambda)\colon F(u, \lambda, \alpha^*) = 0\}$$

in a neighbourhood of (u^*, λ^*).

Apart from *corank*, there is another nonnegative integer called *codimension* (abbrev. *codim*) that is related to each singular point from the classification list. It measures its complexity (in a sense): A singular point with a finite *codim* may appear generically provided that the dimension k of the imperfection parameter $\alpha \in \mathbf{R}^k$ satisfies $k \geqslant codim$. We refer to [2] for details.

Let us call the singular points that are classified via [2] as *bifurcation singularities*.

The simpliest bifurcation singularity is a *turning point* (labelled also as a *limit point*). It has $codim = 0$ and $corank = 1$. The techniques of its computation has been developed some fifteen years ago, see e.g. [9], [10], [14], [12], [18], [11], [3].

Given a fixed imperfection $\alpha \in \mathbf{R}^k$, turning points are regular roots $(u, \lambda) \in \mathbf{R}^N \times \mathbf{R}^1$ of particular *extended systems* $H(u, \lambda, \alpha) = 0$, where $H(\cdot, \cdot, \alpha): \mathbf{R}^N \times \mathbf{R}^1 \to \mathbf{R}^N \times \mathbf{R}^1$,

$$H(u, \lambda, \alpha) = \begin{pmatrix} F(u, \lambda, \alpha) \\ \sigma(u, \lambda, \alpha) \end{pmatrix}, \tag{1.1}$$

provided that $\sigma(u, \lambda, \alpha) \in \mathbf{R}^1$ *factors through* $\det F_u(u, \lambda, \alpha)$.

In this paper, we consider the extended system proposed in [3]: We choose and fix *bordering matrices* $L \in \mathscr{L}(\mathbf{R}^N, \mathbf{R}^1)$ and $M \in \mathscr{L}(\mathbf{R}^1, \mathbf{R}^N)$, and define the (open) set

$$\mathfrak{D} = \left\{ (u, \lambda, \alpha) \in \mathbf{R}^N \times \mathbf{R}^1 \times \mathbf{R}^k : \det \begin{pmatrix} F_u(u, \lambda, \alpha) & M \\ L & 0 \end{pmatrix} \neq 0 \right\}. \tag{1.2}$$

Finally, given $(u, \lambda, \alpha) \in \mathfrak{D}$, we define $\sigma \in \mathbf{R}^1$ as the $(N+1)$st component of the solution to the linear system

$$\begin{pmatrix} F_u(u, \lambda, \alpha) & M \\ L & 0 \end{pmatrix} \begin{pmatrix} w \\ \sigma \end{pmatrix} = \begin{pmatrix} 0 \\ 1 \end{pmatrix}, \quad w \in \mathbf{R}^N, \quad \sigma \in \mathbf{R}^1. \tag{1.3}$$

By virtue of the Implicit Function Theorem, $\sigma: \mathbf{R}^N \times \mathbf{R}^1 \times \mathbf{R}^k \to \mathbf{R}^1$ is a smooth function on $\mathfrak{D}$. It is also easy to check that $\det F_u(u, \lambda, \alpha) = C(u, \lambda, \alpha)\, \sigma(u, \lambda, \alpha)$ where $C(u, \lambda, \alpha) \neq 0$ on $\mathfrak{D}$. It can be shown, see Remark 2.5 in §2, that $(u, \lambda, \alpha) \in \mathfrak{D}$ is a turning point of F if and only if

$$H(u, \lambda, \alpha) = 0, \quad \dim \operatorname{Ker} H_{u,\lambda}(u, \lambda, \alpha) = 0, \tag{1.4}$$

i.e., (u, λ) is a regular root of $H(\cdot, \cdot, \alpha): \mathbf{R}^{N+1} \to \mathbf{R}^{N+1}$.

Remark 1.1. Many other extended systems for turning points (see e.g. [12] for *direct methods*) can be presented in a similar fashion. For example, taking $M := F_\lambda(u, \lambda, \alpha)$ as a (no longer fixed) bordering matrix, we get σ and H that correspond to the method proposed in [14]. It is also possible to use singular value decomposition of $F_u(u, \lambda, \alpha)$ in order to define (variable) bordering marices M and L, etc. We claim that the results of this paper do not depend essentially on the particular technique applied for the construction of H.

It is clear that any bifurcation singularity $(u^*, \lambda^*, \alpha^*) \in \mathfrak{D}$ is a root of $H(\cdot, \cdot, \alpha^*)$. If *codim* of the singularity exceeds 0 then $(u^*, \lambda^*, \alpha^*)$ is no longer a regular root namely,

$$H(u^*, \lambda^*, \alpha^*) = 0, \quad \dim \operatorname{Ker} H_{u,\lambda}(u^*, \lambda^*, \alpha^*) \geqslant 1.$$

In such a case, given a small imperfection $z \in \mathbf{R}^k$, we fix $\alpha = \alpha^* + z$. The mapping $H(\cdot, \cdot, \alpha)\colon \mathbf{R}^N \times \mathbf{R}^1 \to \mathbf{R}^{N+1}$ possesses a finite set of (generically) *regular* roots (these are, in fact, *turning points* of $F(\cdot, \cdot, \alpha)$) that cluster in a neighbourhood of (u^*, λ^*). The particular scenario is supplied by the theory for imperfect bifurcation, [2].

The objective of this paper is a global analysis of Newton method for finding the roots of $H(\cdot, \cdot, \alpha)$ assuming that a particular bifurcation singularity $(u^*, \lambda^*, \alpha^*)$ is specified as an *organizing center*.

Given an imperfection $z \in \mathbf{R}^k$, we set $\alpha = \alpha^* + z$ and define a vector field $\mathcal{N}(\cdot, \cdot, \alpha)\colon \mathbf{R}^N \times \mathbf{R}^1 \to \mathbf{R}^N \times \mathbf{R}^1$,

$$\mathcal{N}(u, \lambda, \alpha) = -(H_{u,\lambda}(u, \lambda, \alpha))^{-1} H(u, \lambda, \alpha). \tag{1.5}$$

Let us call it *Newton vector field*. Obviously, the domain of $\mathcal{N}(\cdot, \cdot; \cdot)$ should be restricted to $\mathfrak{D}$. It contains a neighbourhood of the organizing center $(u^*, \lambda^*, \alpha^*)$. Moreover, the vector field $\mathcal{N}(\cdot, \cdot; \alpha^* + z)$ degenerates on the critical set

$$\mathfrak{C}_{\mathcal{N}}(z) \equiv \{(u, \lambda)\colon \det H_{u,\lambda}(u, \lambda, \alpha^* + z) = 0\}. \tag{1.6}$$

We shall consider (both classical and damped) *Newton iterations*

$$\begin{pmatrix} u^{(n+1)} \\ \lambda^{(n+1)} \end{pmatrix} = \begin{pmatrix} u^{(n)} \\ \lambda^{(n)} \end{pmatrix} + d\,\mathcal{N}(u^{(n)}, \lambda^{(n)}, \alpha^* + z), \tag{1.7}$$

where $d > 0$ is a damping parameter. Newton iterations are a discrete version of the *continuous Newton method*, i.e., the initial value problem for the system of ordinary differential equations

$$\begin{pmatrix} \dot{u}(t) \\ \dot{\lambda}(t) \end{pmatrix} = \mathcal{N}(u(t), \lambda(t), \alpha^* + z), \quad \begin{pmatrix} u(0) \\ \lambda(0) \end{pmatrix} = \begin{pmatrix} u^{(0)} \\ \lambda^{(0)} \end{pmatrix}. \tag{1.8}$$

The relevant flow $\varphi(\cdot, t)$ on $(\mathbf{R}^N \times \mathbf{R}^1) \setminus \mathfrak{C}_{\mathcal{N}}(z)$, defined as $\varphi(u^{(0)}, \lambda^{(0)}, t) \equiv (u(t), \lambda(t))$, is called *Newton flow* for the operator (1.1) where $\alpha = \alpha^* + z$. The fact that φ depends smoothly on parameter $z \in \mathbf{R}^k$ will be reflected by the notation $\varphi(\cdot, t; z)$.

It is well known that Newton iterations (1.7) can be interpreted as the Euler discretisation (with a step-size equal to d) of the solution trajectory $(u(t), \lambda(t))_{t \geqslant 0}$ to (1.8). The importance of the continuous Newton method consists in the fact that

it can be analysed comparatively easier then its discrete versions. Simultaneously, the qualitative information concerning the behavior of the Newton flow is quite significant for understanding the discrete version (1.7) of the method.

The regular roots of $H(\cdot,\cdot,\alpha^*+z)=0$, $z\neq 0$, are *local attractors* for any of the above mentioned versions of Newton method. Precisely speaking, the regular roots are *stable nodes* (see e.g. [4, p. 147]) of

a) the field $\mathcal{N}(\cdot,\cdot,\alpha^*+z)$ as far as the dynamical system (1.8) is concerned

b) the relevant iteration map related to (1.7).

Note that except for the roots of $H(\cdot,\cdot,\alpha^*+z)$, there are *no* fixed points (i.e., steady states) of the field $\mathcal{N}(\cdot,\cdot,\alpha^*+z)$ on a sufficiently small neighbourhood of (u^*,λ^*) (minus $\mathfrak{C}_{\mathcal{N}}(z)$, of course), for each z sufficiently small in modulus.

The aim of this paper is a global analysis of the *basins of attraction* for the methods (1.7–8):

Definition 1.2. Given an imperfection $z\in\mathbf{R}^k$, let (u,λ) be a fixed point of the vector field $\mathcal{N}(\cdot,\cdot,\alpha^*+z)$ on $\mathbf{R}^N\times\mathbf{R}^1$. The set $\mathfrak{B}_{\mathcal{N}}(u,\lambda;z)\equiv\{(u^{(0)},\lambda^{(0)})\in\mathbf{R}^N\times\mathbf{R}^1\colon \varphi(u^{(0)},\lambda^{(0)},t;z)\to(u,\lambda)$ in $\mathbf{R}^N\times\mathbf{R}^1$ as $t\to+\infty\}$ is called the basin of attraction of the fixed point (u,λ) for the continuous Newton method (1.8). Similarly, $\mathfrak{B}^d_{\mathcal{N}}(u,\lambda;z)\equiv\{(u^{(0)},\lambda^{(0)})\in\mathbf{R}^N\times\mathbf{R}^1$: the sequence $\{(u^{(n)},\lambda^{(n)})\}_{n=0}^{+\infty}$ generated by (1.7) converges to (u,λ) in $\mathbf{R}^N\times\mathbf{R}^1$ as $n\to+\infty\}$ is the basin of attraction of the point (u,λ) for the (damped) Newton method (1.7) with damping parameter d.

In [1], there was suggested to *regularise* the Newton field $\mathcal{N}$, see (1.5), by a suitable rescaling: Let $\mathcal{N}^r(\cdot,\cdot,\alpha)\colon\mathbf{R}^N\times\mathbf{R}^1\to\mathbf{R}^N\times\mathbf{R}^1$ be defined as

$$\mathcal{N}^r(u,\lambda,\alpha)=n(u,\lambda,\alpha)\cdot\mathcal{N}(u,\lambda,\alpha),\quad n(u,\lambda,\alpha)\equiv\det H_{u,\lambda}(u,\lambda,\alpha) \tag{1.9}$$

for each $(u,\lambda,\alpha)\in\mathfrak{D}$. (In order to get the idea, consider the inverse $(H_{u,\lambda}(u,\lambda,\alpha))^{-1}$ in (1.5) calculated via Cramer's rule). Let $\varphi^r(\cdot,t,z)$ be the flow related to the regularised Newton field $\mathcal{N}^r(\cdot,\cdot,\alpha^*+z)\colon\mathbf{R}^{N+1}\to\mathbf{R}^{N+1}$. Its domain is obviously the slice

$$\mathfrak{D}_z\equiv\{(u,\lambda)\in\mathbf{R}^N\times\mathbf{R}^1\colon(u,\lambda,\alpha^*+z)\in\mathfrak{D}\}.$$

Remark 1.3. The flows $\varphi(\cdot,t;z)$ and $\varphi^r(\cdot,t,;z)$ are *topologically equivalent* (up to, perhaps, a time reverse) on connected components of $\mathfrak{D}_z\setminus\mathfrak{C}_{\mathcal{N}}(z)$. The reverse of time is required on those components where $n(u,\lambda,\alpha)<0$.

Remark 1.4. The (regular) roots $(u,\lambda)\in\mathfrak{D}_z\setminus\mathfrak{C}_{\mathcal{N}}(z)$, $z\neq 0$, of $H(\cdot,\cdot,\alpha^*+z)=0$ are also fixed points of the regularised Newton field $\mathcal{N}(\cdot,\cdot,\alpha^*+z)$ namely, they are *stable* and *unstable nodes* respectively, provided that $n(u,\lambda,\alpha^*+z)$ is *positive* and *negative*. Setting $n(u,\lambda,\alpha)\equiv-\det H_{u,\lambda}(u,\lambda,\alpha)$ in (1.9), the characterisation of the nodes (*stable/unstable*) is reversed.

Remark 1.5. Apart from the mentioned fixed points on $\mathfrak{D}_z \setminus \mathfrak{C}_{\mathcal{N}}(z)$ *additional* fixed points of $\mathcal{N}^r(\cdot, \cdot, \alpha^* + z)$ should be admitted on $\mathfrak{C}_{\mathcal{N}}(z)$. These may have substantional influence on the global convergence properties of both (1.7) and (1.8).

One way to understand the global convergence properties of Newton method goes back to the results by JULIA and FATOU. These indicate that boundaries of the basins of attraction may reproduce themselves. This property of *self-similarity* suggests some links with *fractal geometry*. So far, a rigorous theory may be provided for mappings subjected to very restrictive assumptions. Most of the research in this direction is based on computer assisted studies. Let us quote e.g. [13], [16] as stimulating examples of an effort in this direction.

Another concept is to apply Singularity Theory. In [8], the *generic bifurcation singularities* of the regularised Newton flow $\mathcal{N}^r$ on the critical set are analysed. (The relevant $H: \mathbb{R}^N \to \mathbb{R}^N$ is assumed to be a potential mapping with $N = 2$ and $N = 3$). It yields flow patterns for $\varphi(\cdot, t)$ in a neighbourhood the fixed points on the critical set that persist a perturbation of the mapping. This kind of analysis gives a *quasiglobal* information (in the sense of an unfolded normal form).

Our analysis tries to extend the information taking into account the parameter-dependent flow between *all* fixed points of $\mathcal{N}^r$ that are locally available. We have not applied the concept of *genericity* and, instead, we assume a particular scenario that describes the splitting of a multiple root to H into a set of simple roots when H is subjected to a small perturbation. The crucial role plays Center Manifold(-like) Theorem for the Newton flow. All these concepts were outlined in [5] assuming a special case of the organizing center (namely, a *simple bifurcation point*). The aim of this presentation is an attempt for a generalisation.

The fact that H is a rather particular mapping (an extended system for turning points) does not seem to be a substantional restriction of our analysis. We believe that the technique may be applied as soon as a *genesis* (i.e., an *organizing center*) of simple roots to H is defined by the usual means of the Singularity Theory.

2. Dimensional reduction

The function $\sigma: \mathbb{R}^N \times \mathbb{R}^1 \times \mathbb{R}^k \to \mathbb{R}^1$ defined in (1.3), is closely related to a version of Ljapunov-Schmidt dimensional reduction of the mapping $F: \mathbb{R}^N \times \mathbb{R}^1 \times \mathbb{R}^k \to \mathbb{R}^N$:

We recall the fixed bordering vectors L and M, and the set $\mathfrak{D}$, see (1.2). Given $(u, \lambda, \alpha) \in \mathfrak{D}$ and $(x, s, z) \in \mathbb{R}^1 \times \mathbb{R}^1 \times \mathbb{R}^k$, we require $g \in \mathbb{R}^1$ and $v \in \mathbb{R}^N$ to satisfy

$$\begin{aligned} F(u + v, \lambda + s, \alpha + z) - Mg &= F(u, \lambda, \alpha) \\ Lv &= x \end{aligned} \tag{2.1}$$

Obviously, $g = 0 \in \mathbf{R}^1$ and $v = 0 \in \mathbf{R}^N$ solve (2.1) at the origin $(x, s, z) = 0 \in \mathbf{R}^{2+k}$.

As a consequence of Implicit Function Theorem, the conditions (2.1) define g and v as germs of smooth mappings $g: \mathbf{R}^1 \times \mathbf{R}^1 \times \mathbf{R}^k \to \mathbf{R}^1$ and $v: \mathbf{R}^1 \times \mathbf{R}^1 \times \mathbf{R}^k \to \mathbf{R}^N$ centred at the origin. Moreover, both g and v depend smoothly on $(u, \lambda, \alpha) \in \mathfrak{D}$ as a parameter i.e., $g = g(x, s, z; u, \lambda, \alpha)$ and $v = v(x, s, z; u, \lambda, \alpha)$. Writing $g(0; u, \lambda, \alpha)$ or $v(0; u, \lambda, \alpha)$, we mean the part (x, s, z) of the relevant argument to be $0 \in \mathbf{R}^{2+k}$. The same convention is understood for the partial differentials of g and v.

Definition 2.1. Let us say that $g = g(x, s, z; u, \lambda, \alpha)$ defined by (2.1), is the reduction of the mapping F at the point $(u, \lambda, \alpha) \in \mathfrak{D}$.

Partial differentials of $g = g(x, s, z; u, \lambda, \alpha)$ and $v = v(x, s, z; u, \lambda, \alpha)$ with respect to $(x, s, z) \in \mathbf{R}^{2+k}$ and $(u, \lambda, \alpha) \in \mathbf{R}^N \times \mathbf{R}^{1+k}$ can be obtained from (2.1) by implicit differentiation (and chain rule, as far as higher differentials are concerned). For example, g_x, v_x and g_s, v_s at $(x, s, z; u, \lambda, \alpha)$ are defined by the solution to the following linear systems

$$(2.2) \qquad \begin{pmatrix} F_u & M \\ L & 0 \end{pmatrix} \begin{pmatrix} v_x \\ -g_x \end{pmatrix} = \begin{pmatrix} 0 \\ 1 \end{pmatrix} \quad , \quad \begin{pmatrix} F_u & M \\ L & 0 \end{pmatrix} \begin{pmatrix} v_s \\ -g_s \end{pmatrix} = - \begin{pmatrix} F_\lambda \\ 0 \end{pmatrix}$$

where F_u and F_λ are evaluated at $(u + v(x, s, z; u, \lambda, \alpha), \lambda + s, \alpha + z) \in \mathbf{R}^N \times \mathbf{R}^{1+k}$.

In principle, any differential of g and v can be computed at the cost of the numerical solution of (a canonical sequence of) linear problems with the same matrix $F_u(u + v, \lambda + s, \alpha + z)$ being augmented by the column vector M and the row vector L, see the definition of $\mathfrak{D}$. Let us note that $v = v(x, s, z; u, \lambda, \alpha)$ is not known explicitly except for $(x, s, z) = 0$. If $(x, s, z) \neq 0$, the value of $v(x, s, z; u, \lambda, \alpha)$ has to be computed numerically from the nonlinear equation (2.1) via Newton iterations, see [5], Remark 3.2.

Remark 2.2. The function $\sigma: \mathbf{R}^N \times \mathbf{R}^1 \times \mathbf{R}^k \to \mathbf{R}^1$, see (1.3) and (1.1), is related to the reduction g of the mapping F as follows:

$$(2.3) \qquad \sigma(u, \lambda, \alpha) = g_x(0; u, \lambda, \alpha)$$

for each $(u, \lambda, \alpha) \in \mathfrak{D}$.

Proposition 2.3. *If* $(u, \lambda, \alpha) \in \mathfrak{D}$ *then*

$$\dim \operatorname{Ker} H_{u,\lambda}(u, \lambda, \alpha) = \dim \operatorname{Ker} \begin{pmatrix} g_x(0; u, \lambda, \alpha) & g_s(0; u, \lambda, \alpha) \\ g_{xx}(0; u, \lambda, \alpha) & g_{xs}(0; u, \lambda, \alpha) \end{pmatrix}.$$

Proof. Direct calculations yield that $\xi \in \mathbf{R}^{N+1}$ belongs to $\operatorname{Ker} H_{u,\lambda}(u,\lambda,\alpha)$ if and only if $\xi = v_x(0;u,\lambda,\alpha)\delta x + v_s(0;u,\lambda,\alpha)\delta s$, where δx, $\delta s \in \mathbf{R}^1$ satisfy

$$\begin{pmatrix} g_x(0;u,\lambda,\alpha) & g_s(0;u,\lambda,\alpha) \\ g_{xx}(0;u,\lambda,\alpha) & g_{xs}(0;u,\lambda,\alpha) \end{pmatrix} \begin{pmatrix} \delta x \\ \delta s \end{pmatrix} = \begin{pmatrix} 0 \\ 0 \end{pmatrix}.$$

□

Bifurcation singularities of F on $\mathfrak{D}$ can be classified as the roots $(u^0,\lambda^0,\alpha^0) \in \mathfrak{D}$ of F that satisfy additional set of scalar conditions that represent requirements on certain partial derivatives $\frac{\partial^{p+q}}{\partial x^p \partial s^q} g(x,s,z;u^0,\lambda^0,\alpha^0)$ of the reduction $g = g(x,s,z;u,\lambda,\alpha)$ at $(x,s,z) = 0 \in \mathbf{R}^{2+k}$ and $(u,\lambda,\alpha) = (u^0,\lambda^0,\alpha^0)$.

As examples, we list definitions of particular bifurcation singularities that will be considered as organizing centers $(u^*,\lambda^*,\alpha^*) \in \mathfrak{D}$ of the mapping H, see (1.1) and (2.3).

Definition 2.4. A point $(u^0,\lambda^0,\alpha^0) \in \mathfrak{D}$ is a **turning point** provided that $F(u^0,\lambda^0,\alpha^0) = 0$, and

$$g_x(0;u^0,\lambda^0,\alpha^0) = 0, \tag{2.4}$$

$$g_{xx}(0;u^0,\lambda^0,\alpha^0) \neq 0, g_s(0;u^0,\lambda^0,\alpha^0) \neq 0. \tag{2.5}$$

Remark 2.5. It follows from (2.3), Definition 2.5 and Proposition 2.3 that (u,λ,α) is a turning point of F if and only if (u,λ) is a regular root of $H(\cdot,\cdot,\alpha)$: $\mathbf{R}^{N+1} \to \mathbf{R}^{N+1}$, see (1.4).

Definition 2.6. A point $(u^0,\lambda^0,\alpha^0) \in \mathfrak{D}$ is a **simple bifurcation** point (and **isola formation center**, respectively), provided that $F(u^0,\lambda^0,\alpha^0) = 0$, and

$$g_x(0;u^0,\lambda^0,\alpha^0) = g_s(0;u^0,\lambda^0,\alpha^0) = 0, \tag{2.6}$$

(2.7)
$$g_{xx}(0;u^0,\lambda^0,\alpha^0) \neq 0,$$
$$g_{xx}(0;u^0,\lambda^0,\alpha^0) g_{ss}(0;u^0,\lambda^0,\alpha^0) - g_{xs}^2(0;u^0,\lambda^0,\alpha^0) > 0 \quad (< 0, \text{ respectively}).$$

Definition 2.7. A point $(u^0,\lambda^0,\alpha^0) \in \mathfrak{D}$ is a **hysteresis** point provided that $F(u^0,\lambda^0,\alpha^0) = 0$, and

$$g_x(0;u^0,\lambda^0,\alpha^0) = g_{xx}(0;u^0,\lambda^0,\alpha^0) = 0, \tag{2.8}$$

(2.9) $$g_{xxx}(0;u^0,\lambda^0,\alpha^0)\neq 0, g_s(0;u^0,\lambda^0,\alpha^0)\neq 0.$$

Definition 2.8. A point $(u^0,\lambda^0,\alpha^0)\in\mathfrak{D}$ is a **pitchfork bifurcation** point provided that $F(u^0,\lambda^0,\alpha^0)=0$ and

(2.10) $$g_x(0;u^0,\lambda^0,\alpha^0)=g_s(0;u^0,\lambda^0,\alpha^0)=g_{xx}(0;u^0,\lambda^0,\alpha^0)=0,$$

(2.11) $$g_{xxx}(0;u^0,\lambda^0,\alpha^0)\neq 0, g_{xs}(0;u^0,\lambda^0,\alpha^0)\neq 0.$$

Definition 2.9. A point $(u^0,\lambda^0,\alpha^0)\in\mathfrak{D}$ is an **asymmetric cusp** point provided that $F(u^0,\lambda^0,\alpha^0)=0$ and

(2.12) $$\begin{aligned} &g_x(0;u^0,\lambda^0,\alpha^0)=g_s(0;u^0,\lambda^0,\alpha^0)=0,\\ &g_{xx}(0;u^0,\lambda^0,\alpha^0)g_{ss}(0;u^0,\lambda^0,\alpha^0)-g_{xs}^2(0;u^0,\lambda^0,\alpha^0)=0,\end{aligned}$$

(2.13) $$g_{xx}(0;u^0,\lambda^0,\alpha^0)\neq 0, \frac{\mathrm{d}^3}{\mathrm{d}t^3}g(t\beta,t,0,u^0,\lambda^0,\alpha^0)\,|_{t=0}\neq 0,$$

where $\beta=-g_{xs}(0;u^0,\lambda^0,\alpha^0)/g_{xx}(0;u^0,\lambda^0,\alpha^0)$.

Remark 2.10. The above definitions are *independent* of the particular reduction (i.e., the choice of the bordering vectors L and M). It follows essentially from [6].

Remark 2.11. The bifurcation singularities quoted above have *corank* = 1. In principle, singularities (u^*,λ^*,α^*) with *corank* $\geqslant 2$ could not be used as *organizing centers* of the particular H on $\mathfrak{D}$. The reason is that $(u^*,\lambda^*,\alpha^*)\notin\mathfrak{D}$ whatever choice of bordering *vectors* L and M were considered since $\dim\operatorname{Ker}F_u(u^*,\lambda^*,\alpha^*)=$ *corank* $\geqslant 2$.

Each bifurcation singularity (u^*,λ^*,α^*) of F is linked (via a dimensional reduction to the *bifurcation equation* $g(x,s,0;u^*,\lambda^*,\alpha^*)=0$, and via a *contact equivalence* on the ring of germs of smooth mappings $\mathbf{R}^1\times\mathbf{R}^1\to\mathbf{R}^1$) to a *normal form* $\mathfrak{h}$: $\mathbf{R}^1\times\mathbf{R}^1\to\mathbf{R}^1$ of the particular singularity, see [2]. The equation $\mathfrak{h}(x,s)=0$ describes qualitative features of the *(perfect) bifurcation diagram* $\mathscr{S}$ of F, see the introduction in §1.

Refering to [2] again, there exists a *universal unfolding*

$$h:\mathbf{R}^1\times\mathbf{R}^1\times\mathbf{R}^{codim}\to\mathbf{R}^1$$

of the normal form $\mathfrak{h}$ related to each bifurcation singularity with a finite *codim*. The universal unfolding has the following property: If the fixed imperfection parameter α^*

is subjected to a small (in modulus) perturbation $z \in \mathbf{R}^k$ then there exists $\tilde{z} \in \mathbf{R}^{codim}$ such that the *imperfect bifurcation diagram*, i.e., the solution set

$$\mathscr{S}_z = \{(u, \lambda) \in \mathbf{R}^N \times \mathbf{R}^1 : F(u, \lambda, \alpha^* + z) = 0\},$$

of $F(\cdot, \cdot, \alpha^* + z)$ can be linked (via a local diffeomorphism) with the solution set (imperfect bifurcation diagram)

$$\mathfrak{S}_{\tilde{z}} = \{(x, s) \in \mathbf{R}^2 : h(x, s, \tilde{z}) = 0\}$$

of $h(\cdot, \cdot, \tilde{z})$. It is important to note that the mentioned local diffeomorphism linkes the turning points of $F(\cdot, \cdot, z)$ with the turning points of $h(\cdot, \cdot, \tilde{z})$. The statement has the obvious local meaning.

The mapping $\mathscr{Z} : \mathbf{R}^k \to \mathbf{R}^{codim}$ that relates $\tilde{z} \equiv \mathscr{Z}(z)$ to a given imperfection $z \in \mathbf{R}^k$ is defined and smooth on a neighbourhood of the origin $0 \in \mathbf{R}^k$. Obviously, $\mathscr{Z}(0) = 0$.

This mapping may become a local diffeomorphism. In this case we say that $F : \mathbf{R}^N \times \mathbf{R}^1 \times \mathbf{R}^k \to \mathbf{R}^N$ is *universal unfolding* of $F(\cdot, \cdot, \alpha^*)$ at the singular point $(u^*, \lambda^*, \alpha^*)$. Necessarily, $k = codim$. For example, in case of *hysteresis point* $(u^*, \lambda^*, \alpha^*) \in \mathbf{R}^N \times \mathbf{R}^1 \times \mathbf{R}^1$, the sufficient condition for F to be a universal unfolding reads as follows, see [2], Chapter 3:

$$\det \begin{pmatrix} g_x(0; u^*, \lambda^*, \alpha^*), & g_s(0; u^*, \lambda^*, \alpha^*), & g_z(0; u^*, \lambda^*, \alpha^*) \\ g_{xx}(0; u^*, \lambda^*, \alpha^*), & g_{xs}(0; u^*, \lambda^*, \alpha^*), & g_{xz}(0; u^*, \lambda^*, \alpha^*) \\ g_{xxx}(0; u^*, \lambda^*, \alpha^*), & g_{xxs}(0; u^*, \lambda^*, \alpha^*), & g_{xxz}(0; u^*, \lambda^*, \alpha^*) \end{pmatrix} \neq 0. \tag{2.14}$$

Due to (2.8–9), the condition (2.14) can be obviously reformulated namely,

$$g_s(0; u^*, \lambda^*, \alpha^*)\, g_{xz}(0; u^*, \lambda^*, \alpha^*) - g_z(0; u^*, \lambda^*, \alpha^*)\, g_{xs}(0; u^*, \lambda^*, \alpha^*) \neq 0. \tag{2.15}$$

In the case of a general bifurcation singularity $(u^*, \lambda^*, \alpha^*)$ with $corank = 1$, a sufficient condition can be formulated analogously.

In the following Table, universal unfoldings of the normal forms to the above selected bifurcation singularities are reviewed:

Table 2.12. Universal unfoldings $h : \mathbf{R}^1 \times \mathbf{R}^1 \times \mathbf{R}^{codim} \to \mathbf{R}^1$ of normal forms:

nomenclature	*codim*	$h = h(x, s, z),\ z \in \mathbf{R}^{codim}, \lvert p\rvert = \lvert q\rvert = 1$
simple bif. point	1	$p(x^2 - s^2) + z$
isola form. center	1	$p(x^2 + s^2) + z$
hysteresis	1	$px^3 + qs + xz$
pitchfork	2	$px^3 + qxs + z_1 + x^2 z_2$
asymmetric cusp	2	$px^2 + qs^3 + z_1 + sz_2$

Let $(u^*, \lambda^*, \alpha^*) \in \mathbf{R}^N \times \mathbf{R}^1 \times \mathbf{R}^k$ be a particular bifurcation singularity (say, from the above list). Let us set $k = codim$. The problem is to characterise the imperfections $z \in \mathbf{R}^k$ that yield only *regular roots* of $H(\cdot, \cdot, \alpha^* + z) = 0$, provided that we restrict them to a fixed (independent of z) neighbourhood of (u^*, λ^*). Refering to Proposition 2.3, a root $(u, \lambda) \in \mathbf{R}^{N+1}$ of $H(\cdot, \cdot, \alpha^* + z) = 0$, satisfying $(u, \lambda, \alpha^* + z) \in \mathfrak{D}$, is *singular* provided that either $g_s(0; u^*, \lambda^*, \alpha^* + z) = 0$ or $g_{xx}(0; u^*, \lambda^*, \alpha^* + z) = 0$. It motivates to define

$$\mathscr{B} \equiv \{(u, \lambda, \alpha) \in \mathfrak{D} \colon F(u, \lambda, \alpha) = 0, \quad g_x(0; u, \lambda, \alpha) = 0, \quad g_s(0; u, \lambda, \alpha) = 0\}$$

and

$$\mathscr{H} \equiv \{(u, \lambda, \alpha) \in \mathfrak{D} \colon F(u, \lambda, \alpha) = 0, \quad g_x(0; u, \lambda, \alpha) = 0, \quad g_{xx}(0; u, \lambda, \alpha) = 0\}.$$

In accordance with [2], Chapter 3, let us call them *bifurcation* and *hysteresis set*, respectively. We refer to Definition 2.6 and Definition 2.7 for a motivation. The structure of $\mathscr{B}$ and $\mathscr{H}$ may be very complicated (unpredictable, in fact) unless we restrict them to a fixed, sufficiently small neighbourhood $\mathfrak{N}^* \subset \mathfrak{D}$ of the chosen bifurcation singularity $(u^*, \lambda^*, \alpha^*) \in \mathfrak{D}$. Thus, we set

$$\mathscr{H}^* = \mathscr{H} \cap \mathfrak{N}^*, \quad \mathscr{B}^* = \mathscr{B} \cap \mathfrak{N}^*.$$

Let $\mathscr{B}^*_{imp}$ and $\mathscr{H}^*_{imp}$ be the natural projections of $\mathscr{B}^*$ and $\mathscr{H}^*$ into the space $\mathbf{R}^k$ of imperfection parameters α.

Definition 2.13. The subset $\mathscr{B}^*_{imp} \cup \mathscr{H}^*_{imp}$ of $\mathbf{R}^k$ is called **transition set**. The simply connected components of the complement to the transition set are called **regularity regions**.

We can (formally) answer the above posed question: Given z from a regularity region, the equation $H(u, \lambda, \alpha^* + z) = 0$ resticted to the slice

$$\mathfrak{N}^*_z \equiv \{(u, \lambda) \in \mathbf{R}^N \times \mathbf{R}^1 \colon (u, \lambda, \alpha^* + z) \in \mathfrak{N}\},$$

has only regular roots (u, λ). The converse statement is also at hand. Moreover, the number of roots in $\mathfrak{N}^*_z$ is *constant* when z are selected from the *same* regularity region. In [2], Chapter 3, there is shown that the imperfect bifurcation diagrams $\mathscr{S}_z$, being restricted to the slice $\mathfrak{N}^*_z$, are "qualitatively the same" (counting, e.g., the number of turning points) for all z from the same regularity region.

There is a natural conjecture related to our analysis of Newton iterations:

Conjecture 2.14. *Each regularity region determines one particular global convergence pattern of Newton method. For example, given two imperfections z_1 and z_2 from the same regularity region, the Newton flows $\varphi(\cdot, t; z_i)$ on $\mathfrak{N}_{z_i}$ are expected to be topologically equivalent.*

3. Newton flow

We assume $(u^*, \lambda^*, \alpha^*) \in \mathfrak{D}$ to be a singular point with *corank* $= 1$, see Remark 2.11. The aim of this Section is to rewiev results concerning properties of the Newton flow $\varphi(\cdot, t; z)$, see (1.8). Essentially, we shall follow [5]. Let us note that in [5], there was assumed $(u^*, \lambda^*, \alpha^*)$ to be a particular bifurcation singularity namely, a simple bifurcation point, see Definition 2.6. We claim that the below quoted results rely (unless explicitly stated) only on the assumption that $(u^*, \lambda^*, \alpha^*) \in \mathfrak{D}$ has *corank* $= 1$.

Given an imperfection $z \in \mathbf{R}^k$ sufficiently small in modulus, there exists a 2-dimensional invariant manifold of the Newton flow. The manifold contains all the roots of the extended system $H(\cdot, \cdot, \alpha^* + z) = 0$ that are "organized" by the singular point (u^*, λ^*). In order to formulate the result, we recall g and v, see (2.1), and set

$$g(x, s, z) \equiv g(x, s, z; u^*, \lambda^*, \alpha^*), \quad v(x, s, z) \equiv v(x, s, z; u^*, \lambda^*, \alpha^*).$$

Theorem 3.1. *Let $z \in \mathbf{R}^k$ be a sufficiently small (in modulus) imperfection. The set*

$$\mathfrak{I}(z) \equiv \{(u, \lambda) \in \mathbf{R}^N \times \mathbf{R}^1 : u = u^* + v(x, s, z), \quad \lambda = \lambda^* + s, \quad (x, s) \in \mathbf{R}^2\}$$

is invariant manifold of the Newton flow $\varphi(\cdot, t; z) : \mathbf{R}^N \times \mathbf{R}^1 \to \mathbf{R}^N \times \mathbf{R}^1$.

Proof. We refer to [5], Theorem 3.5. The proof consists in a straightforward computation of the field $\mathcal{N}(\cdot, \cdot, \alpha^* + z)$ restricted to $\mathfrak{I}(z)$. It can be shown that

$$\mathcal{N}(u^* + v(x, s, z), \lambda^* + s, \alpha^* + z) = \begin{pmatrix} v_x(x, s, z)\delta x + v_s(x, s, z)\delta s \\ \delta s \end{pmatrix} \tag{3.1}$$

where δx, $\delta s \in \mathbf{R}^1$ are the solution to

$$\begin{pmatrix} g_x(x, s, z) & g_s(x, s, z) \\ g_{xx}(x, s, z) & g_{xs}(x, s, z) \end{pmatrix} \begin{pmatrix} \delta x \\ \delta s \end{pmatrix} = - \begin{pmatrix} g(x, s, z) \\ g_x(x, s, z) \end{pmatrix}. \tag{3.2}$$

□

Theorem 3.2. *There exist neighbourhoods* $\mathfrak{U}$ *and* $\mathfrak{V}$ *of* $(u^*, \lambda^*) \in \mathbf{R}^N \times \mathbf{R}^1$ *and the origin* $0 \in \mathbf{R}^2$ *such that it holds: Given a sufficiently small (in modulus) imperfection* $z \in \mathbf{R}^k$, *a point* $(u, \lambda) \in \mathfrak{U}$ *satisfies* $H(u, \lambda, \alpha^* + z) = 0$, *see (1.1) and (2.3), if and only if* $(u, \lambda) \in \mathfrak{I}(z)$, *i.e.,* $u = u^* + v(x, s, z)$ *and* $\lambda = \lambda^* + s$, *where* $(x, s) \in \mathfrak{V}$ *solves*

$$g(x, s, z) = 0, \quad g_x(x, s, z) = 0. \tag{3.3}$$

Proof. For, see [5], Theorem 3.4. □

Obviously, the flow $\varphi(\cdot, t; z)$ on the invariant manifold $\mathfrak{I}(z)$ can be described in coordinates $(x, s) \in \mathbf{R}^2$ that parametrise $\mathfrak{I}(z)$. In particular, (3.1) and (3.2) motivate to define a vector field $\mathscr{M}(\cdot, z) \colon \mathbf{R}^2 \to \mathbf{R}^2$,

$$\mathscr{M}(x, s, z) = -\begin{pmatrix} g_x(x, s, z) & g_s(x, s, z) \\ g_{xx}(x, s, z) & g_{xs}(x, s, z) \end{pmatrix}^{-1} \begin{pmatrix} g(x, s, z) \\ g_x(x, s, z) \end{pmatrix}. \tag{3.4}$$

Let $\psi(\cdot, t; z) \colon \mathbf{R}^2 \to \mathbf{R}^2$, $t \in \mathbf{R}^1$, be the flow related to the vector field $\mathscr{M}(\cdot, z)$ on $\mathbf{R}^2$. We say that ψ is *reduced Newton flow.*

In fact, $\varphi(\cdot, t; z)$ is defined on $(\mathbf{R}^N \times \mathbf{R}^1) \setminus \mathfrak{C}_{\mathscr{N}}(z)$, see (1.6). Similarly, $\psi(\cdot, t; z)$ is virtually a flow on $\mathbf{R}^2 \setminus \mathfrak{C}_{\mathscr{M}}(z)$, where $\mathfrak{C}_{\mathscr{M}}(z) = \{(x, s) \colon m(x, s, z) = 0\}$ and

$$m(x, s, z) \equiv \det \begin{pmatrix} g_x(x, s, z) & g_s(x, s, z) \\ g_{xx}(x, s, z) & g_{xs}(x, s, z) \end{pmatrix}. \tag{3.5}$$

We will have this fact in mind whenever we would say that $\psi(\cdot, t; z)$ is a flow on $\mathbf{R}^2$.

Corollary 3.3. *Given an imperfection* $z \in \mathbf{R}^k$, *the flows* $\varphi(\cdot, t; z) \colon \mathfrak{I}(z) \to \mathfrak{I}(z)$ *and* $\psi(\cdot, t; z) \colon \mathbf{R}^2 \to \mathbf{R}^2$ *are topologically equivalent (conjugate), see e.g. [4, Definition 1.7.3, p. 38] for this notion.*

We can formally define a discrete version to the flow $\psi(\cdot, t; z)$ with a fixed imperfection z: Given (x^0, s^0) as an initial approximation of a turning point of $g(\cdot, \cdot, z)$, see (3.3), we define the classical/damped Newton iterations

$$\begin{pmatrix} x^{(n+1)} \\ s^{(n+1)} \end{pmatrix} = \begin{pmatrix} x^{(n)} \\ s^{(n)} \end{pmatrix} + d.\mathscr{M}(x^{(n)}, s^{(n)}, z), \tag{3.6}$$

where $d = 1$ / $d > 0$ is a damping parameter.

It should be emphasized that discrete approximations of φ (namely, Newton iterations (1.7)) do *not* leave $\mathfrak{I}(z)$ *invariant.* Consequently, the iterations (3.6) have no clear link with the "large scale" iterations (1.7). Nevertheless, it is shown in [5] that

(3.6) can be implemented as a fairly reasonable numerical method for determining the roots of $H(\cdot,\cdot,\alpha^*+z)$.

Let us come back to the original subject namely, to the Newton flow. The significance of the reduced flow ψ follows from a Center Manifold (-like) Theorem, we are going to formulate. For that purpose, we have to introduce new coordinates in $\mathbf{R}^N \times \mathbf{R}^1$.

First, we define an auxiliary projection operator $Q \in \mathscr{L}(\mathbf{R}^N, \mathbf{R}^N)$ setting $Q = I - (M^\top M)^{-1} MM^\top$. Note that $\operatorname{Ker} Q = \operatorname{span}\{M\}$ and $\dim \operatorname{Im} Q = N - 1$. If $(u,\lambda,\alpha) \in \mathfrak{D}$ then it is easy to check that the linear operator $QF_u(u,\lambda,\alpha)\colon \{u \in \mathbf{R}^N : Lu = 0\} \to \operatorname{Im} Q$ is regular. Given $w \in \operatorname{Im} Q$ and $(x,s,z) \in \mathbf{R}^{2+k}$, let $V \in \mathbf{R}^N$ and $(\lambda,\alpha) \in \mathbf{R}^{1+k}$ satisfy

$$QF(u^*+V,\lambda^*+s,\alpha^*+z) = w, \quad LV = x, \quad \lambda = \lambda^*+s, \quad \alpha = \alpha^*+z.$$

The Implicit Function Theorem yields that $V = V(w,x,s,z)$ is a germ of a smooth mapping.

The mapping $\mathscr{R}\colon \operatorname{Im} Q \times \mathbf{R}^2 \times \mathbf{R}^k \to \mathbf{R}^N \times \mathbf{R}^1 \times \mathbf{R}^k$ defined as

$$\mathscr{R}(w,x,s,z) = (u,\lambda,\alpha), \quad u = u^* + V(w,x,s,z), \lambda = \lambda^* + s, \alpha = \alpha^* + z$$

is a local diffeomorphism. It is also clear that domain of $\mathscr{R}^{-1}$ can be extended to $\mathfrak{D}$. We refer to each point $\mathscr{R}^{-1}(u,\lambda,\alpha)$ by giving the level w of $QF(u,\lambda,\alpha)$, the scalar quantity $x = Lu - Lu^*$ and the shift (s,z) of parameters (λ,α) w.r.t. (λ^*,α^*).

Given $z \in \mathbf{R}^k$, we define a flow $\omega(\cdot,t;z)$ on $\operatorname{Im} Q \times \mathbf{R}^2$ that is conjugate to the flow $\varphi(\cdot,t;z)$ on $\mathbf{R}^N \times \mathbf{R}^1$ setting

$$\omega((w,x,s),t;z) \equiv \mathscr{R}^{-1}(\varphi(\mathscr{R}(w,x,s,z),t;z),\alpha^*+z)$$

for $(w,x,s,z) \in \mathscr{R}^{-1}(\mathfrak{D})$.

Theorem 3.4. *The flow $\omega(\cdot,\tau;z)$ corresponds to the dynamical system*

$$\dot{w} = -w \tag{3.7}$$

$$\begin{pmatrix} \dot{x} \\ \dot{s} \end{pmatrix} = \mathscr{F}(w,x,s,z), \tag{3.8}$$

where $\mathscr{F}(\cdot,\cdot,\cdot,z)\colon \operatorname{Im} Q \times \mathbf{R}^2 \to \mathbf{R}^2$ is a smooth mapping on $(\operatorname{Im} Q \times \mathbf{R}^2) \setminus \mathscr{R}^{-1}(\mathfrak{C}_{\mathscr{M}}(z), \alpha^*+z)$ for each sufficiently small perturbation $z \in \mathbf{R}^k$. The operator $\mathscr{F}$ is a smooth perturbation of the vector field $\mathscr{M}$, see (3.4), namely,

$$\mathscr{F}(0,\cdot,\cdot,z) \equiv \mathscr{M}(\cdot,\cdot,z).$$

Proof. We refer to [5], Theorem 6.6, where $\mathscr{F}$ is also explicitly defined. □

It is simple to elucidate that $\mathfrak{I}(z)$ is $\mathscr{R}(\cdot,\cdot,\cdot,z)$-image of the subspace $\{(w,x,s)\in \operatorname{Im} Q\times\mathbf{R}^2\colon w=0\}$. Any phase curve of the system (3.7–8) is exponentially attracted by the mentioned subspace, unless it hits the critical set $\mathscr{R}^{-1}(\mathfrak{C}_{\mathscr{F}}(z),\alpha^*+z)$. Consequently, the invariant manifold $\mathfrak{I}(z)$ plays the same role of an attracting set as far as Newton flow $\varphi(\cdot,t;z)$ is concerned.

The natural conjecture is that the right-hand side of (3.8) should be replaced by (3.4) namely,

Conjecture 3.5. *If $z\neq 0$ then the flow $\omega(\cdot,t;z)$ is topologically equivalent to* (3.7),

$$\begin{pmatrix}\dot{x}\\ \dot{s}\end{pmatrix}=\mathscr{M}(x,s,z). \tag{3.9}$$

It seems that the reduced Newton flow $\psi(\cdot,t;z)$ on $\mathbf{R}^2$ may be significant of the "large scale" flow $\varphi(\cdot,t;z)$ on $\mathbf{R}^{N+1}$.

We shall go on analysing $\psi(\cdot,t;z)$. It is clear that properties of this 2-dimensional, parameter dependent flow stem from properties of the singular point (u^*,λ^*,α^*). This point is assumed to be classified as a particular bifurcation singularity with finite *codim* (and *corank* = 1). In particular, we shall consider those from Definitions 2.4–9 in this paper. We also assume F to be an universal unfolding of $F(\cdot,\cdot,\alpha^*)$ at (u^*,λ^*,α^*), see §2. Consequently, $k=$ *codim*. Then turning points of $g(\cdot,\cdot,z)$ for a given imperfection $z\in\mathbf{R}^k$, i.e., the roots of (3.3) are linked with turning points of the relevant universal unfolding $h(\cdot,\cdot,\tilde{z})\colon \mathbf{R}^1\times\mathbf{R}^1\to\mathbf{R}^1$ of the normal form $\mathfrak{h}$ that is related to the particular bifurcation singularity (u^*,λ^*,α^*), see Table 2.12 for examples. The imperfection $\tilde{z}$ is related to the given z via a local diffeomorphism $\mathscr{Z}$.

Let $\mathscr{M}^*(\cdot,z)\colon\mathbf{R}^2\to\mathbf{R}^2$ be the version of the vector field $\mathscr{M}(\cdot,z)$, see (3.4), where g is replaced by the above unfolding h, i.e.,

$$\mathscr{M}^*(x,s,z)=-\begin{pmatrix}h_x(x,s,z) & h_s(x,s,z)\\ h_{xx}(x,s,z) & h_{xs}(x,s,z)\end{pmatrix}^{-1}\begin{pmatrix}h(x,s,z)\\ h_x(x,s,z)\end{pmatrix}. \tag{3.10}$$

Let $\psi^*(\cdot,t;z)$ be the relevant flow on $\mathbf{R}^2$ that is defined by the vector field $\mathscr{M}^*(\cdot,z)$. One may think that both flows $\psi(\cdot,t;z)$ and $\psi^*(\cdot,t;\mathscr{Z}(z))$ may perform similarly:

Conjecture 3.6. *Given $z\in\mathbf{R}^k$ sufficiently small in modulus, the flows $\psi(\cdot,t;z)$ and $\psi^*(\cdot,t;\mathscr{Z}(z))$ are topologically equivalent on a sufficiently small neighbourhood of the origin $0\in\mathbf{R}^2$.*

In one particular case, the above conjecture has been verified:

Theorem 3.7. *Let $(u^*, \lambda^*, \alpha^*)$ be a simple bifurcation point, see Definition 2.6. Let $k = 1$ and let F be a universal unfolding of $F(\cdot, \cdot, \alpha^*)$ at $(u^*, \lambda^*, \alpha^*)$, see §2. Let us set $p = \operatorname{sgn} g_{xx}(0)$ in the relevant formula for the unfolding $h = p(x^2 - s^2) + z$, see Table 2.12. Then there exist neighbouhoods $\mathfrak{U}$ and $\mathfrak{U}^*$ of the origin $0 \in \mathbb{R}^3$ such that the flow $\psi(\cdot, \tau; z)$ on the slice $\mathfrak{U}_z = \{(x, t) \in \mathbb{R}^2 : (x, t, z) \in \mathfrak{U}\}$ and the flow $\psi^*(\cdot, \tau; Z)$ on the slice $\mathfrak{U}_Z^* = \{(x, t) \in \mathbb{R}^2 : (x, t, Z) \in \mathfrak{U}^*\}$ are topologically equivalent provided that both imperfections z and Z are sufficiently small in modulus and satisfy*

$$\operatorname{sgn} g_x(0) \operatorname{sgn} z = \operatorname{sgn} Z. \tag{3.11}$$

Proof. Cf. [5], Theorem 5.1. The assertion concerning the *topological equivalence* means that there exists a homeomorphism $\mathfrak{U}_z \to \mathfrak{U}_Z^*$ taking all trajectories of the flow $\psi(\cdot, t; z)$ onto those of $\psi^*(\cdot, t; Z)$. The homeomorphism preserves orientation of the trajectories but it does not preserve necessarily the parametrisation by time t. □

Let us note that the assumption (3.11) embraces the requirement $Z = \mathscr{Z}(z)$, compare with Conjecture 3.6, as a special case. For a detailed reasoning, see [5].

Remark 3.8. We claim that the statement of Theorem 3.7 remains true if $(u^*, \lambda^*, \alpha^*)$ were *isola formation center*. The proof of the above quoted Theorem 5.1 in [5] can be easily adapted since universal unfoldings of both simple bifurcation point and isola formation center differ up to a change of one sign, see Table 2.12.

In the coming sections §4–§6, we present three case studies concerning *hysteresis*, *pitchfork* and *asymmetric cusp* to be the organizing centers for both Newton flow and Newton iterations. We shall question the above formulated Conjectures 3.6, 3.5 and 2.14.

At the end of this Section, we shall recall some technicalities from [5] that are concerned with analyzing the reduced Newton flow ψ. Finally, we mention a regularised version of the flow ψ and give its interpretation as a locally Hamiltonian flow on $\mathbb{R}^2$. As an important byproduct, we gain a useful tool for numerical experiments with the phase portraits of ψ.

Given an imperfection $z \in \mathbb{R}^k$, let us consider a mapping $\mathscr{T}(\cdot; z) : \mathbb{R}^2 \to \mathbb{R}^2$ defined as

$$\mathscr{T}(x, s; z) = (g(x, s, z), g_x(x, s, z))^{\mathsf{T}} \equiv (\xi, \eta)^{\mathsf{T}}. \tag{3.12}$$

Obviously, $\mathscr{T}(\cdot; z)$ is a local diffeomorphism on $\mathbb{R}^2 \setminus \mathfrak{C}_{\mathscr{M}}(z)$.

Observation 3.9. *The image* $(\xi(t), \eta(t)) = \mathscr{T}(x(t), s(t); z)$ *of any trajectory* $(x(t), s(t)) \equiv \psi(\cdot, t; z)$ *satisfies*

$$\dot{\xi} = -\xi \quad , \quad \dot{\eta} = -\eta. \tag{3.13}$$

Note that trajectories of (3.13) are oriented rays directed towards the origin $0 \in \mathbb{R}^2$. Thus, images of trajectories $\psi(\cdot, t; z)$ are the mentioned rays *restricted* to the image of the x, s-space (a neighbourhood of the origin) via the mapping $\mathscr{T}(\cdot; z)$. The crucial point of the analysis consists in a specification of the domain of a (possibly) multivalued inverse $\mathscr{T}^{-1}(\cdot; z)$. We shall exploit this idea in §4.

Following (1.9), we may regularise the field $\mathscr{M}$. Let us elaborate: Setting

$$\mathscr{M}^r(x, s, z) \equiv m(x, s, z).\mathscr{M}(x, s, z), \tag{3.14}$$

where $m = m(x, s, z)$ is defined in (3.5), we obtain a smooth vector field $\mathscr{M}^r(\cdot, z)$ on a fixed neighbourhood of the origin $0 \in \mathbb{R}^2$ for each sufficiently small imperfection $z \in \mathbf{R}^k$. Let $\psi^r(\cdot, t; z)$ be the flow defined by the field $\mathscr{M}^r(\cdot, z)$ on $\mathbb{R}^2$ (in the obvious local sense). Note that the flows $\psi(\cdot, t; z)$ and $\psi^r(\cdot, t; z)$ are *topologically* identical in $\mathbf{R}^2 \setminus \mathbb{C}_{\mathscr{M}}(z)$. Namely, all the trajectories of $\psi(\cdot, t; z)$ are taken to those of $\psi^r(\cdot, t; z)$ up to a nonsmooth time-rescaling that preserves the orientation at those points (x, s) of the phase space where $m(x, s, z) > 0$ and reverses the orientation when $m(x, s, z) < 0$.

The properties of the phase curves related to the flow (3.13) suggest that the ratio

$$\mathbf{H}(x, s, z) \equiv \frac{g_x(x, s, z)}{g(x, s, z)} \tag{3.15}$$

should be *constant* along any phase curve of the flow $\psi(\cdot, t; z)$ on $\mathbb{R}^2 \setminus \mathbb{C}_{\mathscr{M}}(z)$ and, consequently, the flow $\psi^r(\cdot, t; z)$ on $\mathbb{R}^2$. It is easy to verify the following

Observation 3.10. *The flow* $\psi^r(\cdot, t; z)$ *on* $\mathbb{R}^2 \setminus \{(x, s) \in \mathbb{R}^2 : g(x, s, z) = 0\}$ *is defined by the dynamical system*

$$\begin{pmatrix} \dot{x} \\ \dot{s} \end{pmatrix} = g^2(x, s, z) \begin{pmatrix} -\mathbf{H}_s(x, s, z) \\ \mathbf{H}_x(x, s, z) \end{pmatrix} \tag{3.16}$$

In other words, the phase portraits of the flow $\psi^r(\cdot, t; z)$ correspond locally to a Hamiltonian flow on $\mathbf{R}^2$ except for the solutions set to $g(\cdot, \cdot, z) = 0$. The relevant Hamiltonian is $\mathbf{H}(\cdot, \cdot, z)$, see (3.15).

Note that the reciprocal value to $\mathbf{H}(x, s, z)$ is also Hamiltonian of the flow $\psi^r(\cdot, t; z)$ on $\mathbf{R}^2$ except for the set $\{(x, s) \in \mathbf{R}^2 : g_x(x, s, z) = 0\}$.

Remark 3.11. The phase curves of $\psi^r(\cdot, t; z)$ can be simply computed as the *level sets* of $\mathbf{H}(\cdot, \cdot, z)$. In particular, the solution sets to $g(\cdot, \cdot, z) = 0$ and to $g_x(\cdot, \cdot, z) = 0$ interpreted as the level sets $\mathbf{H}(\cdot, \cdot, z) = 0$ and $\mathbf{H}^{-1}(\cdot, \cdot, z) = 0$ respectively, are (a union of) phase curves of $\psi^r(\cdot, \cdot, z)$.

Remark 3.12. In the obvious local sense it holds: The flow $\psi^r(\cdot, t; z)$ is Hamiltonian in a neighbourhood of the point (x^0, s^0) provided that either $g(x^0, s^0, z) \neq 0$ or $g_x(x^0, s^0, z) \neq 0$.

We recall that a *hyperbolic* fixed point of a planar Hamiltonian flow is either a **saddle point** or a **center**. Consequently, saddles and centers are the fixed points of $\psi^r(\cdot, t; z)$ to be generically encountered on $\mathfrak{C}_{\mathscr{M}}(z)$ for imperfections $z \neq 0$. This simple reasoning yields the same result that was already achieved in [8] in a slightly different context (see our comment in §1).

4. A case study: hysteresis

Let $(u^*, \lambda^*, \alpha^*) \in \mathfrak{D}$ be a *hysteresis point*, see Definition 2.7. Moreover, we assume $F(\cdot, \cdot, \alpha^* + z)$ to be *universal unfolding* of $F(\cdot, \cdot, \alpha^*)$, i.e., we assume $k = 1$ and (2.15).

We shall discuss Conjecture 3.6 in this context. In order to be particular, let us fix $p = 1$ and $q = -1$ in the universal unfolding $h = h(x, s, z)$ of the relevant normal form, see Table 2.12. Given an imperfection $z \in \mathbb{R}^1$, we consider the vector field $\mathscr{M}^*(\cdot, z)$, see (3.10), and its regularised version $\mathscr{M}^{*r}(\cdot, z)$ that is defined in the spirit of (3.14). The relevant flows are $\psi^*(\cdot, t; z)$ and $\psi^{*r}(\cdot, t; z)$ respectively.

Fig. 4.1, Fig. 4.2 and Fig. 4.3 depict the phase portraits of ψ^{*r} with imperfections $z = 0$, $z = -0.05$ and $z = 0.05$. The thick solid line (that is actually the s-axis) represents the critical set $\mathfrak{C}_{\mathscr{M}^*}(z)$ for the relevant z. Note that the phase curves of $\psi^*(\cdot, t; z)$ are identical with those of $\psi^{*r}(\cdot, t; z)$ except for the critical set where the former phase curves are not defined and up to, perhaps, the orientation (since $pq = -1$, $\operatorname{sgn} m(x, s, z) = -pq \operatorname{sgn} x = \operatorname{sgn} x$ i.e., the arrows in the half-plane $\{(x, s): x < 0\}$ should be reversed). It is important to point out that $\mathfrak{C}_{\mathscr{M}^*}(0)$ is also a phase curve of the flow $\psi^{*r}(\cdot, t; 0)$. It consists of *fixed points* of the field $\mathscr{M}^{*r}(\cdot, 0)$.

The local diffeomorphism $\mathscr{Z}$ quoted in Conjecture 3.6 preserves the origin, i.e., $\mathscr{Z}(0) = 0$. At first, we shall question Conjecture 3.6 just in the special case that $z = 0 \in \mathbb{R}^1$.

Let us set $g(x, s, z) \equiv h(x, s, z) + \gamma x s^2$, where $\gamma \in \mathbb{R}^1$ is a parameter. It can be readily verified that g satisfies (2.8–9) and (2.15) for any choice of parameter γ. Fixing a value of γ, we define $\mathscr{M}(x, s, z)$ and $\mathscr{M}^r(x, s, z)$, see (3.4) and (3.14). As usual, ψ and ψ^r are the relevant, z-parameter dependent flows. Moreover, they depend implicitly on the choice of γ as well. Due to Conjecture 3.6, the flows

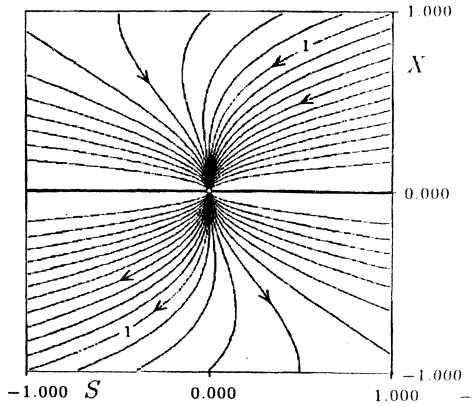

Fig. 4.1

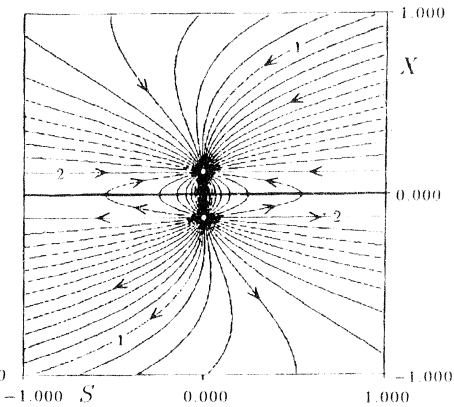

Fig. 4.2

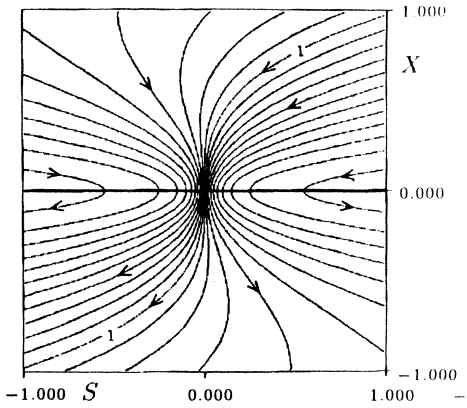

Fig. 4.3

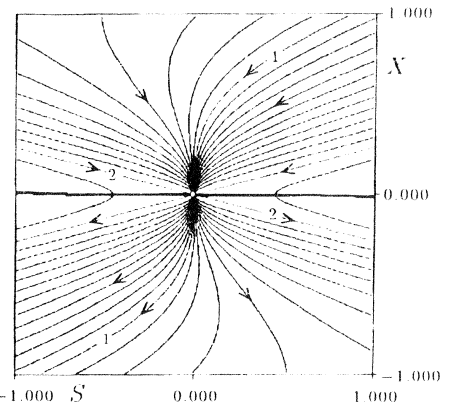

Fig. 4.4

$\psi(\cdot,t;0)$ and $\psi^r(\cdot,t;0)$ respectively, should be topologically equivalent to $\psi^*(\cdot,t;0)$ and $\psi^{*r}(\cdot,t;0)$ whatever choice of γ were concerned.

On Fig. 4.4 and Fig. 4.7, the phase portraits of $\psi^r(\cdot,t;0)$ are plotted assuming two comparatively small values of γ namely, $\gamma = -0.2$ and $\gamma = 0.2$, respectively. At the first glimpse, the flows on Fig. 4.1, Fig. 4.4 and Fig. 4.7 are topologically different: On Fig. 4.4, we observe two hyperbolic and two parabolic regions of the flow in a neighbourhood of the origin $0 \in \mathbf{R}^2$. On the contrary, the flow from Fig. 4.7 exhibits two elliptic regions and two parabolic regions. In general, given any γ, the origin is a ***nonhyperbolic (degenerate) fixed point*** of the vector field $\mathscr{H}^r(\cdot,0)$ on $\mathbf{R}^2$. Moreover, if $\gamma \neq 0$ then the origin is an *isolated* fixed point. Its *Poincaré index* is 0 and 2 for $\gamma < 0$ and $\gamma > 0$, respectively. The observed facts contradict the statement of Conjecture 3.6. In other words, the flow patterns on Figs.4.1–3 could not serve as

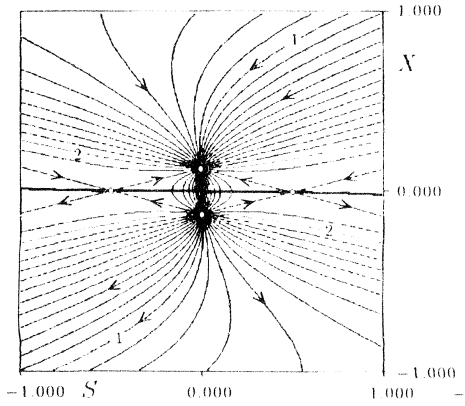

Fig. 4.5

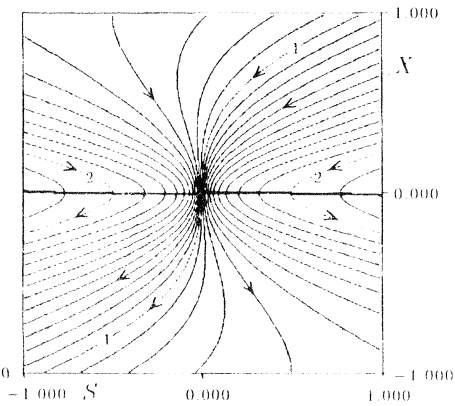

Fig. 4.6

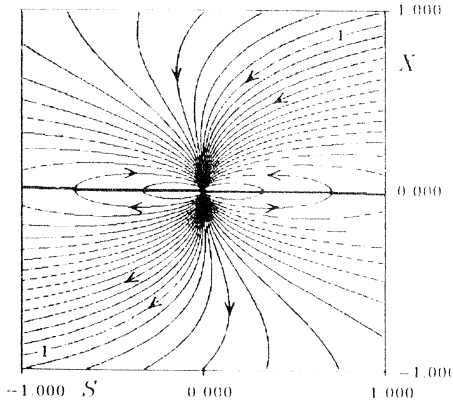

Fig. 4.7

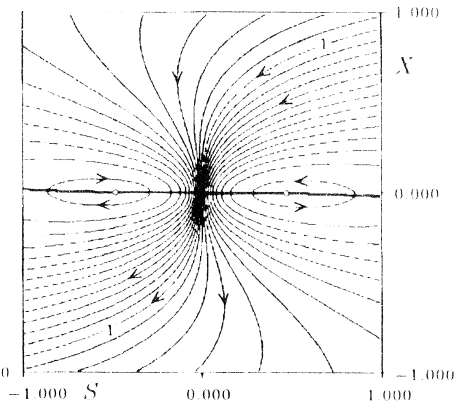

Fig. 4.8

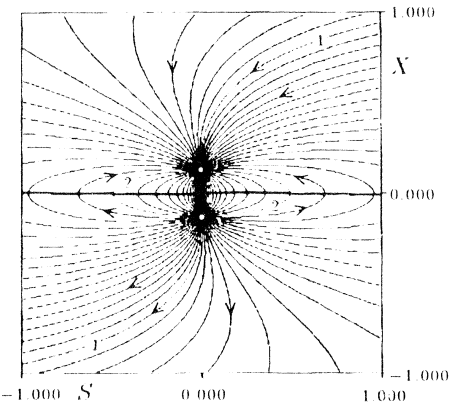

Fig. 4.9

universal prototypes of the reduced Newton flow ψ that is organized by a hysteresis bifurcation point. For example, the flows on Fig. 4.4 and Fig. 4.7, subjected to a perturbation, exhibit qualitatively different behavoir then that offered on Figs.4.2 -3: Fig. 4.5 and Fig. 4.6 report on the phase portrait of the perturbed flow from Fig. 4.4 assuming the imperfection $z = -0.05$ and $z = 0.05$, respectively. Similarly, Fig. 4.8 and Fig. 4.9 yield the same kind of information as far as Fig. 4.7 is concerned. The thick solid curves depict the critical set $\mathfrak{C}_{\mathcal{M}}(z)$ for the relevant z. The special phase curves labeled by 1 and 2 are the solution sets $\{(x,s)\colon g(x,s,z) = 0\}$ and $\{(x,s)\colon g_x(x,s,z) = 0\}$, respectively.

Eventhough Conjecture 3.6 failed, a finite classification of ψ is still available: From now on, we abandon the above counter-examples of g for a while. We consider the flow $\psi(\cdot,t;z)$ related (via (3.4)) to any $g = g(x,s,z) = g(x,s,z;u^*,\lambda^*,\alpha^*)$ that satisfies (2.8–9) and (2.15). We are going to show that the phase portraits on Figs.4.4–9 are significant for the flow of $\psi(\cdot;z)$ provided that g satisfies an additional nondegeneracy Assumption 4.7.

Lemma 4.1. *Given an imperfection $z \neq 0$, the organizing center (hysteresis) degenerates into a pair of limit points if and only if*

$$\operatorname{sgn} z = -\operatorname{sgn} g_{xxx} \operatorname{sgn} g_s \operatorname{sgn} \det \begin{pmatrix} g_s & g_z \\ g_{xs} & g_{xz} \end{pmatrix}, \tag{4.1}$$

where the derivatives of g are to be evaluated at $(x,s,z) = 0 \in \mathbf{R}^3$. If (4.1) is not satisfied then there are no limit points in a neighbourhood of the origin $0 \in \mathbf{R}^2$.

Proof. We refer to Theorem 3.2. Aplying Implicit Function Theorem at the origin $(x,s,z) = 0 \in \mathbf{R}^3$, the solution set to (3.3) can be smoothly parametrised by $x \in \mathbf{R}^1$ namely, a point (x,s,z) solves (3.3) if and only if $z = z^\ell(x)$ and $s = s^\ell(x)$ in the obvious local sense. Implicit differentiation yields

$$\dot{z}^\ell(0) = \dot{s}^\ell(0) = 0, \ddot{z}^\ell(0) = -\frac{g_{xxx} g_s}{\det \begin{pmatrix} g_s & g_z \\ g_{xs} & g_{xz} \end{pmatrix}}. \tag{4.2}$$

The statement (4.1) follows immediately. □

Remark 4.2. Refering to Definition 2.13, the transition set of the hysteresis point consists just of one point $z = 0$. The regularity regions are clearly the sets $\{z \in \mathbf{R}^1\colon z > 0\}$ and $\{z \in \mathbf{R}^1\colon z < 0\}$ restricted to a sufficiently small neighbourhood of the origin.

Let us consider the transformation $\mathscr{T}(\cdot;z)$ on $\mathbb{R}^2$, see (3.12). The strategy of its application is explained in §3.

We shall analyse the image of a fixed, sufficiently small neighbourhood of the origin $0 \in \mathbb{R}^2$ under the mentioned transformation $\mathscr{T}(\cdot;z)$ for small values of z. To this end, we change coordinates on $\mathbb{R}^2$ introducing $\mathscr{T}_0(\cdot;z)\colon \mathbb{R}^2 \to \mathbb{R}^2$,

$$\mathscr{T}_0(x,s;z) = (\mu,s) \quad , \quad \mu = m(x,s,z), \tag{4.3}$$

see (3.5). Note that $m_x = -g_s g_{xxx} \neq 0$ at $(x,s,z) = 0 \in \mathbb{R}^3$. Consequently, $\mathscr{T}_0(\cdot;z)$ is a local diffeomorphism on a fixed neigbourhood of the origin $0 \in \mathbb{R}^2$ assuming small z.

Let us investigate $\mathscr{T}$ in (μ,s)-coordinates, i.e., we define $\mathscr{T}_1(\cdot;z) \equiv \mathscr{T}(\mathscr{T}_0^{-1}(\cdot;z);z)$ on a neighbourhood of the origin $0 \in \mathbb{R}^2$ for small imperfections z. Let us resume that $(\xi,\eta) = \mathscr{T}_1(\mu,s;z)$ if and only if

$$\mu - m(x,s,z) = 0, \quad \xi - g(x,s,z) = 0, \quad \eta - g_x(x,s,z) = 0. \tag{4.4}$$

Note that the first two conditions define implicitly x and s as smooth functions of (μ,ξ,z), i.e.,

$$x = X(\mu,\xi,z), \quad s = S(\mu,\xi,z). \tag{4.5}$$

For, we recall that

$$\det \begin{pmatrix} m_x & m_s \\ g_x & g_s \end{pmatrix} = \det \begin{pmatrix} -g_x g_{xxx} & \cdot \\ 0 & g_s \end{pmatrix} \neq 0$$

at $(x,s,z) = 0$.

Substituting (4.5) into the last condition from (4.4), we obtain

$$\eta - g_x(X(\mu,\xi,z),S(\mu,\xi,z),z) = 0 \tag{4.6}$$

as the *necessary and sufficient condition* for (ξ,η) to be in the range of $\mathscr{T}(\cdot,z)$ in the obvious local sense.

Let us define

$$\eta^c(\xi,z) \equiv g_x(X(0,\xi,z),S(0,\xi,z),z). \tag{4.7}$$

Remark 4.3. The graph of the function $\eta = \eta^c(\xi,z)$ is a local parametrisation of the image $\mathscr{T}(\mathfrak{C}_{\mathscr{M}}(z);z)$ of the critical set $\mathfrak{C}_{\mathscr{M}}(z)$ for sufficiently small z. For, realise that the mentioned function is implicitly defined by (4.4) with $\mu = 0$, eliminating x and ξ.

The leading terms of Taylor expansion

$$\eta^c(\xi, z) = \eta^c_z(0)\, z + \eta^c_\xi(0)\, \xi + \eta^c_{\xi\xi}(0)\, \xi^2 + \mathcal{O}(z^2 + |\xi z| + |\xi^3|) \tag{4.8}$$

depend on the values of selected partial derivatives of g up to the third order computed at the origin $(x, s, z) = 0$. For the sake of completness, let us review the relevant formulae:

$$\begin{aligned} &\eta^c_z(0) = (g_{xz} g_s - g_{xs} g_z)\, g_s^{-1}, \quad \eta^c_\xi(0) = g_{xs} g_s^{-1}, \\ &\eta^c_{\xi\xi}(0) = \frac{1}{2}\,(g^4_{xs} - g_s^2 g^2_{xxs} + g_{xxx} g_s^2 g_{xss}) g_s^{-4} g^{-1}_{xxx}. \end{aligned} \tag{4.9}$$

Note that $\eta^c_z(0) \neq 0$ due to (2.9) and (2.15).

Let us go on analysing (4.6). Expanding (4.6) at $\mu = 0$, it yields

$$\eta - \eta^c(\xi, z) - \mu(g_{xx} X_\mu(0, \xi, z) + g_{xs} S_\mu(0, \xi, z)) - \mu^2(g_{xxx}(0) + R(\mu, \xi, z)) = 0, \tag{4.10}$$

where R is a smooth remainder that vanishes at the origin, and g_{xx}, g_{xs} are to be evaluated at $(x, s, z) = (X(0, \xi, z), S(0, \xi, z), z)$.

We claim that the coefficient at μ in the expansion (4.10) vanishes. Substituting (4.5) into the second equation in (4.4), the implicit differentiation w.r.t. μ at $\mu = 0$ yields $g_x X_\mu + g_s S_\mu = 0$. Since $\mu = 0$, the vector (g_{xx}, g_{xs}) is a multiple of (g_x, g_s), and the claim follows immediately. We may conclude that (4.6) is equivalent to

$$\eta - \eta^c(\xi, z) = \mu^2(g_{xxx}(0) + \mathcal{O}(|\mu| + |\xi| + |z|)) \tag{4.11}$$

for (μ, ξ, z) from a sufficiently small neighbourhood of the origin $0 \in \mathbf{R}^3$.

Lemma 4.4. *For each sufficiently small $\varepsilon > 0$ there exists $\delta > 0$ such that, given any $z \in \mathbf{R}^1$ that satisfies $|z| < \delta$, the pre-image $\mathfrak{U}_z = \mathscr{T}^{-1}(\mathfrak{M}_z; z)$ of the set*

$$\mathfrak{M}_z = \{(\xi, \eta) \in \mathbf{R}^2 : \xi^2 + \eta^2 \leqslant \varepsilon, g_{xxx}(0)\eta \leqslant g_{xxx}(0)\eta^c(\xi, z)\}$$

is an open subset of $\mathbf{R}^2$, containing the origin $0 \in \mathbf{R}^2$. Moreover, denoting the restrictions $\{(x, s) \in \mathfrak{U}_z : m(x, s, z) \geqslant 0\}$ and $\{(x, s) \in \mathfrak{U}_z : m(x, s, z) \leqslant 0\}$ by $\mathfrak{U}_z^+$ and $\mathfrak{U}_z^-$ respectively, we claim that $\mathscr{T}(\cdot; z) : \mathfrak{U}_z^\pm \to \mathfrak{M}_z$ is a **homeomorphism**.

Proof. This simply follows from the above local analysis of the range of $\mathscr{T}(\cdot; z)$, see (4.6), (4.11) and (4.4–5). □

Note that Lemma 4.4 yields the following geometric interpretation of the condition (4.1):

Remark 4.5. Let $z \neq 0$ be sufficiently small in modulus. The condition (4.1) implies that the origin $(\xi, \eta) = 0 \in \mathbf{R}^2$ belongs to the *interior* of $\mathfrak{M}_z$. If (4.1) is not satisfied then the origin stays outside $\mathfrak{M}_z$.

In the above excluded case of $z = 0$, the origin sticks to the boundary $\eta = \eta^c(\xi, 0)$ of $\mathfrak{M}_0$. It follows from (4.8) immediately.

We recall the significance of the flow (3.13). Generically, the phase curves of this flow (recall that these are all oriented rays directed towards the origin) intersect the curve $\eta = \eta^c(\xi, z)$ (i.e. the image $\mathscr{T}(\mathfrak{C}_{\mathscr{M}}(z); z)$) *transversally*. Let us investigate the nongeneric case i.e., the trajectories of (3.13) that are *tangent* to the image of the critical set. The role of these special trajectories will be explained later.

Definition 4.6. Given an imperfection $z \in \mathbf{R}^1$, we say that $(\xi, \eta) \in \mathbf{R}^2$ is a **cross point** of $\mathscr{T}(\mathfrak{C}_{\mathscr{M}}(z); z)$ provided that

(i) $(\xi, \eta) \in \mathscr{T}(\mathfrak{C}_{\mathscr{M}}(z); z)$

(ii) the *tangent* of $\mathscr{T}(\mathfrak{C}_{\mathscr{M}}(z); z)$ at the point (ξ, η) passes through the origin $0 \in \mathbf{R}^2$.

We introduce the following

Assumption 4.7. Let

$$\eta^c_{\xi\xi}(0) \neq 0. \tag{4.12}$$

See (4.9) for the particular conditions upon g at the origin.

By virtue of the above assumption, the function $\eta = \eta^c(\xi, z)$ of ξ is locally either convex or concave for small imperfections z. Consequently, we may give a simple asymptotic description of *cross points*:

Lemma 4.8. *The set*

$$\mathfrak{P} \equiv \{(\xi, \eta, z) \in \mathbf{R}^3 \colon (\xi, \eta) \textit{is a cross point of} \mathscr{T}(\mathfrak{C}_{\mathscr{M}}(z); z)\}$$

is a smooth manifold in a sufficiently small neighbourhood $\mathfrak{N}$ *of the origin* $0 \in \mathbf{R}^3$. *In particular,* $(\xi, \eta, z) \in \mathfrak{P} \cap \mathfrak{N}$ *if and only if*

$$\eta = \eta^c(\xi, z), \quad \eta^c_z(0)z = \eta^c_{\xi\xi}(0)\xi^2 + R(\xi, z) \tag{4.13}$$

where the higher order terms R *behave as* $R(\xi, z) = \mathscr{O}(|\xi z| + z^2 + |\xi^3|)$.

Proof. By definition, (ξ, η) is a cross point provided that $\frac{\partial}{\partial \xi}\eta^c(\xi, z) = \frac{\eta}{\xi} = \frac{\eta^c(\xi, z)}{\xi}$. The rest of the proof consists in a straightforward asymptotic analysis of the resulting equation $\eta^c(\xi, z) = \xi \frac{\partial}{\partial \xi}\eta^c(\xi, z)$, taking (4.8) into account. □

Let us formulate the following corollary:

Remark 4.9. For each sufficiently small $\varepsilon > 0$ there exists $\delta > 0$ such that, given any $z \neq 0$, $|z| < \delta$, there are either *two* or *none* cross points (ξ, η) of $\mathcal{T}(\mathfrak{C}_{\mathcal{M}}(z); z)$ in the circle $\{(\xi, \eta): \xi^2 + \eta^2 < \varepsilon\}$. The former case happens if and only if

$$\operatorname{sgn} z = \operatorname{sgn} \eta_z^c(0) \operatorname{sgn} \eta_{\xi\xi}^c(0). \tag{4.14}$$

The idea is to classify the flow (3.13) on $\mathfrak{M}_z$ for small imperfection z. Note that Lemma 4.4 together with Observation 3.9 relate that flow (via a topological equivalence) to the flow $\psi(\cdot, t; z)$ on $\mathfrak{U}_z^+$ and on $\mathfrak{U}_z^-$.

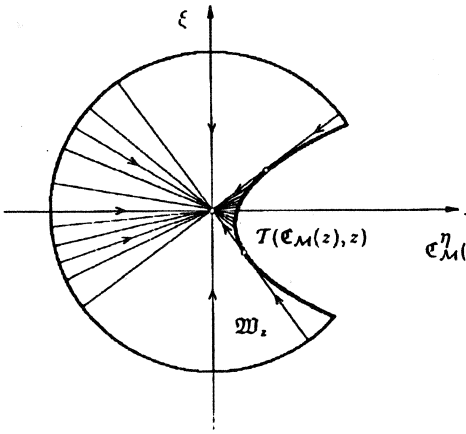

Fig. 4.10a

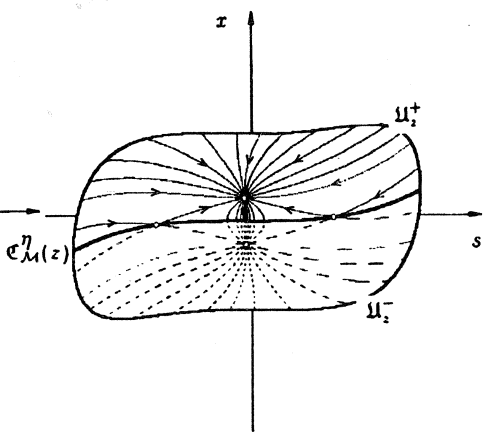

Fig. 4.10b

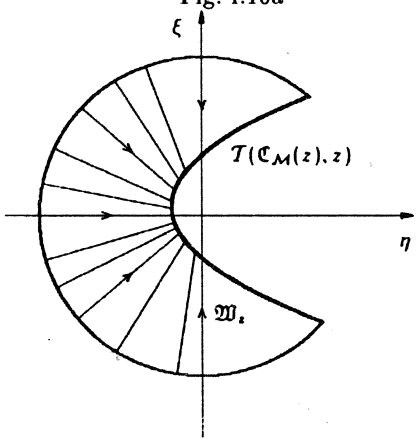

Fig. 4.11a

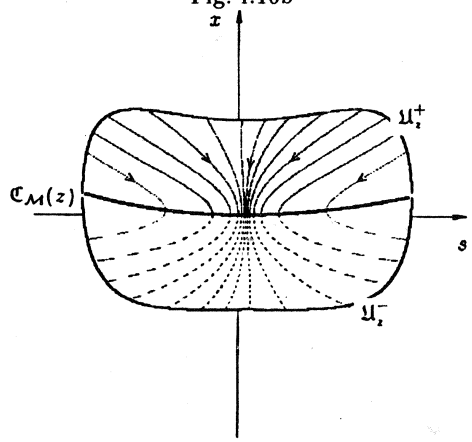

Fig. 4.11b

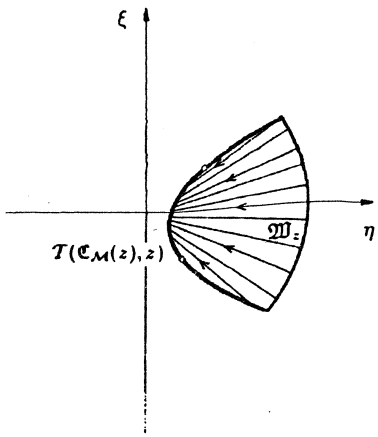

Fig. 4.12a

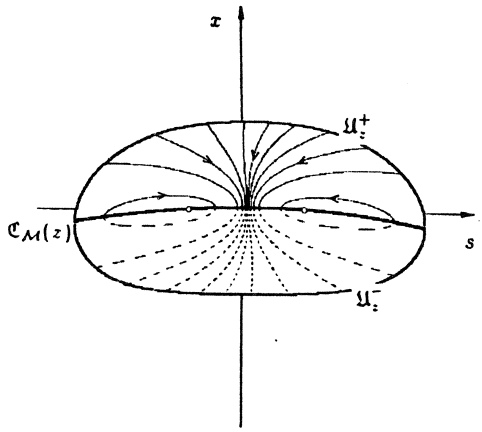

Fig. 4.12b

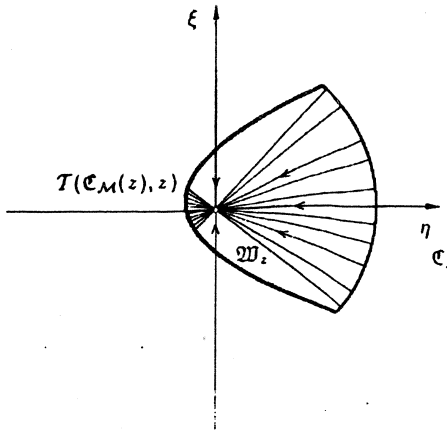

Fig. 4.13a

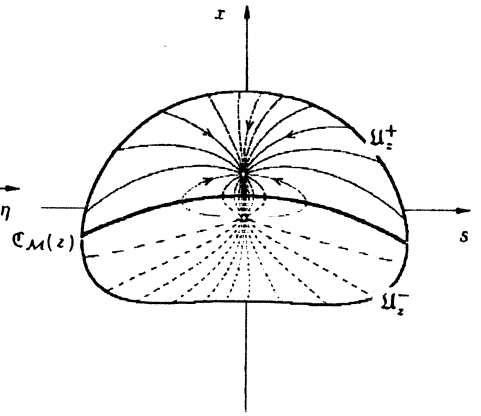

Fig. 4.13b

In order to understand the pictures from Figs.4.10–13, we recall the construction of the phase curves on $\mathfrak{M}_z$: Given a point $(\xi^0, \eta^0) \in \mathfrak{M}_z$,

- take the ray in the (ξ, η)-plane, directed towards the origin and passing through the given point (ξ^0, η^0)
- restrict the ray to $\mathfrak{M}_z$.

The *connected part* of the restriction that contains (ξ^0, η^0) is the trajectory emanating from (ξ^0, η^0).

We refer to Fig. 4.10a, Fig. 4.11a, Fig. 4.12a, and Fig. 4.13a for examples of phase portraits of (3.13) on $\mathfrak{M}_z$. Note that the selected examples of the sets $\mathfrak{M}_z$ cover

all *four* scenarios that are available for small imperfection $z \neq 0$ w.r.t. the conditions (4.1) and (4.14); see Remark 4.5 and Remark 4.9 for the relevant geometric interpretation.

The corresponding phase portraits of $\psi(\cdot, t; z)$ on $\mathfrak{U}_z$ are sketched on Fig. 4.10b, Fig. 4.11b, Fig. 4.12b, and Fig. 4.13b. The dotted trajectories depict the flow on $\mathfrak{U}_z^-$. The link between the flows on $\mathfrak{U}_z^+$ (and $\mathfrak{U}_z^-$, respectively) and the flow on $\mathfrak{M}_z$ is defined via the homeomorphism $\mathscr{T}(\cdot; z)\colon \mathfrak{U}_z^{\pm} \to \mathfrak{M}_z$, cf. Lemma 4.4. The same appeals to $\psi^r(\cdot, t; z)$, changing orientation of the dotted trajectories.

The role of *cross points* becomes clear from Fig. 4.10 and Fig. 4.12. Since the cross points belong to the boundary $\eta = \eta^c(\xi, z)$, each of them has just one pre-image. The pre-images of both cross points from Fig. 4.10a are *saddle points* of the regularised flow $\psi^r(\cdot, t; z)$ on $\mathfrak{U}_z$, see Fig. 4.10b. The alternative interpretation of cross points is on Fig. 4.12: Both pre-images are simultaneously *centres* of $\psi^r(\cdot, t; z)$. Assuming a sufficiently small imperfection $z \neq 0$, we may resume that the flow $\psi^r(\cdot, t; z)$ possess a pair of saddles on $\mathfrak{C}_{\mathscr{M}}(z)$ provided that z satisfies both (4.1) and (4.14). The flow has a pair of centers on $\mathfrak{C}_{\mathscr{M}}(z)$ provided that (4.14) does hold while (4.1) does not. The remaining alternatives for the signum of z imply no fixed points of the flow $\psi^r(\cdot, t; z)$ on $\mathfrak{C}_{\mathscr{M}}(z)$.

If we were to propose a prototype of the flow ψ then it would be related to a "normal form" of g that satisfies Assumption 4.7. The class of the counter-examples analysed at the begining of this Section offers the following candidates: Let us set

$$h(x, s, z, \gamma) = x^3 - s + xz + \gamma x s^2. \tag{4.15}$$

Given any $\gamma \neq 0$, the function $h = h(\cdot, \cdot, \cdot, \gamma)$ (being understood as a germ g) satisfies (2.8–9) and (2.15), as it was already noted. Moreover, the requirement (4.12) can be easily verified.

Let $\psi^*(\cdot, t; z)$ be the flow that is defined by the vector field $\mathscr{M}^*(\cdot; z)$, see (3.10), for the particular h defined in (4.15). The obvious dependence of ψ^* on γ will be reflected by the notation $\psi^*(\cdot, t; z, \gamma)$.

Theorem 4.10. *Let g satisfy* (2.8–9), (2.15) *and* (4.12). *We consider the reduced Newton flow $\psi(\cdot, t; z)$ that is related to g via* (3.4).

Let us choose γ such that

$$\operatorname{sgn} \gamma = \operatorname{sgn}(g_{xxx}(0)\, \eta^c_{\xi\xi}(0)), \tag{4.16}$$

and define $\psi^*(\cdot, t; z, \gamma)$ via (4.15) *and* (3.10). *Then there exist neighbourhoods $\mathfrak{U}$ and $\mathfrak{U}^*$ of the origin $0 \in \mathbf{R}^3$ such that the flow $\psi(\cdot, t; z)$ on the slice $\mathfrak{U}_z = \{(x, t) \in \mathbf{R}^2 : (x, t, z) \in \mathfrak{U}\}$ and the flow $\psi^*(\cdot, t; Z, \gamma)$ on the slice $\mathfrak{U}^*_Z = \{(x, t) \in \mathbf{R}^2 : (x, t, Z) \in \mathfrak{U}^*\}$*

are topologically equivalent provided that both imperfections z and Z are sufficiently small in modulus and satisfy

$$\operatorname{sgn}\left(g_{xxx}(0)\, g_s(0) \det\begin{pmatrix} g_s(0) & g_z(0) \\ g_{xs}(0) & g_{xz}(0) \end{pmatrix}\right) \operatorname{sgn} z = \operatorname{sgn} Z. \tag{4.17}$$

Remark 4.11. As a simple consequence, taking two (sufficiently small) imperfections z_1 and z_2 from the same regularity region, see Remark 4.2, the corresponding flows $\psi(\cdot, t; z_i)$ (and, naturally, $\psi^r(\cdot, t; z_i)$) on $\mathfrak{U}_{z_i}$ will be topologically equivalent. It complies with Conjecture 2.14.

Proof of Theorem 4.10. Let us choose a small $\varepsilon > 0$. We consider a sufficiently small $\delta > 0$ from the assertions of Lemma 4.4, Remark 4.5 and Remark 4.9. We shall treat the case $z \neq 0$ first:

Let $|z| < \delta$. In accordance with Remark 4.5 and Remark 4.9, the relevant set $\mathfrak{M}_z$ can be classified from the following points of view:

(a) $\mathfrak{M}_z$ either does or does not contain the origin

(b) $\mathfrak{M}_z$ contains either two or none cross points.

The particular scenario (out of four alternatives that are available) depends upon whether z does/does not satisfy (4.1) and (4.14). We consider the flow (3.13) on $\mathfrak{M}_z$, and have in mind that it is topologically equivalent to the flow $\psi(\cdot, t; z)$ on $\mathfrak{U}_z^+$ and on $\mathfrak{U}_z^-$, see Lemma 4.4.

The germ $h = h(\cdot, \cdot, \cdot, \gamma)$ is understood as a special choice of g. Let $Z \neq 0$ be an imperfection of h, i.e., $h = h(x, s, Z, \gamma)$. We apply the above treatment to the particular germ: We define $\mathscr{T}^*(\cdot; Z)\colon \mathbf{R}^2 \to \mathbf{R}^2$, $\mathscr{T}^*(x, s; Z) = (h(x, s, Z, \gamma), h_x(x, s, Z, \gamma))^\top$, see (3.12). The relevant versions of Lemma 4.4, Remark 4.5 and Remark 4.9 hold. On the analogy with ε, δ, $\mathfrak{M}_z$ and $\mathfrak{U}_z^\pm$, we define ε^*, δ^*, $\mathfrak{M}_Z^*$ and $\mathfrak{U}_Z^{*\pm}$. We assume $|Z| < \delta^*$. Note that (4.1) and (4.14) read as $\operatorname{sgn} Z = -1$ and $\operatorname{sgn} Z = \operatorname{sgn} \gamma$.

The conditions (4.16–17) gurantee that both $\mathfrak{M}_z$ and $\mathfrak{M}_Z^*$ have the same classification, as far as the above listed criteria (a), (b) are concerned. Then, clearly, the flows (3.13) on $\mathfrak{M}_z$ and on $\mathfrak{M}_Z^*$ are topologically equivalent. Consequently, the flow $\psi(\cdot, t; z)$ on $\mathfrak{U}_z^\pm$ is topologically equivalent to the flow $\psi^*(\cdot, t; Z)$ on $\mathfrak{U}_Z^{*\pm}$. It proves the claim for $z \neq 0$.

The case $z = 0$ can be treated similarly, by linking the flow (3.13) on $\mathfrak{M}_0$ with the same flow restricted to $\mathfrak{M}_0^*$. □

5. A CASE STUDY: PITCHFORK

In this section, we assume $(u^*, \lambda^*, \alpha^*) \in \mathfrak{D}$ to be a *pitchfork bifurcation point*, see Definition 2.8. Let $F(\cdot, \cdot, \alpha^* + z)$ be *universal unfolding* of $F(\cdot, \cdot, \alpha^*)$. Consequently, $k = 2$.

We consider a universal unfolding $h = h(x, s, z_1, z_2)$ of the normal form for a pitchfork bifurcation, see Table 2.12. We choose $p = q = 1$, i.e., $h = x^3 + xs + z_1 + z_2 x^2$. Let $\psi^*(\cdot, t; z)$ be the corresponding Newton flow, and let $\psi^{*r}(\cdot, t; z)$ be its regularised version.

Fig. 5.1 displays the phase portrait of $\psi^{*r}(\cdot, t; 0)$. As a rule, the thick solid curve is the critical set. The particular phase curves that are labeled as 1 and 2 are the solution sets to $g(\cdot, \cdot, z) = 0$ and to $g_x(\cdot, \cdot, z) = 0$, respectively. Unlike in the hysteresis case, the phase portrait seems to be structurally stable w.r.t. the higher order perturbations of $h(\cdot, \cdot, 0)$ that do not change qualitatively the bifurcation diagram (i.e., the pitchfork marked as 1). In other words, Conjecture 3.6 is likely to be true at least for $z = 0 \in \mathbf{R}^2$.

Transition sets (see Definition 2.13) that correspond to the particular germ h can be easily computed. (We refer to [2], Chapter 3, that is the fundamental source of information.) There are four regularity regions. As it was mentioned in §2, each regularity region is characterised by a fixed number of (regular) roots (u, λ) to the equation $H(u, \lambda, \alpha^* + z) = 0$ when z belongs to the particular regularity region. In two regions there is **one** root of $H(\cdot, \cdot, \alpha^* + z) = 0$ guaranteed while in the remaining two regions there are **three** roots available.

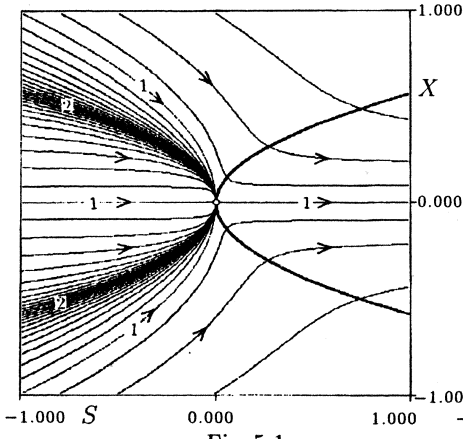

Fig. 5.1

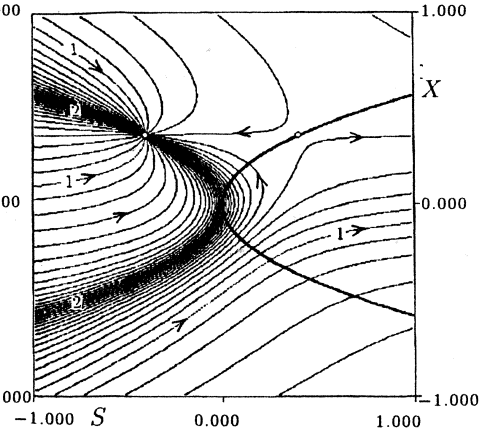

Fig. 5.2

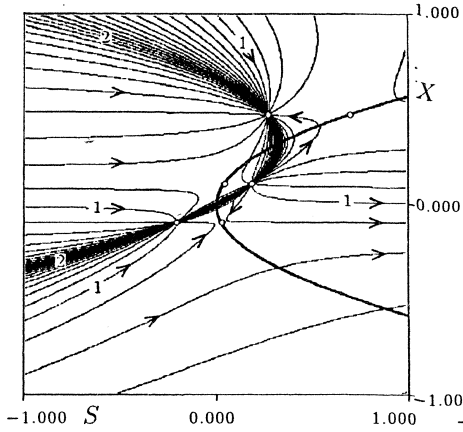

Fig. 5.3

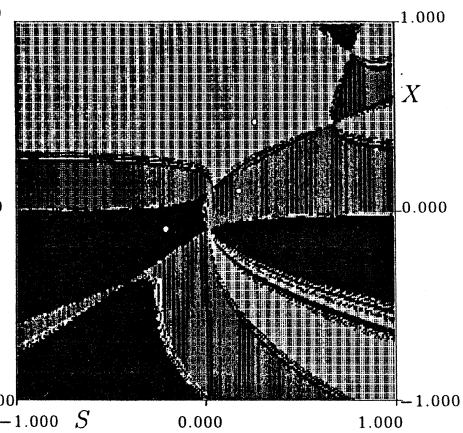

Fig. 5.4

Fig. 5.2 and Fig. 5.3, respectively, present examples of phase portraits of $\psi^{*r}(\cdot, t; z)$, selecting z from the former and the latter kind of regularity region. The particular values of z are $z = (0.1, 0)$ and $z = (-0.01, -1)$, respectively. One can observe additional fixed points (saddles) of the flow $\psi^{*r}(\cdot, t; z)$ on the critical set. The number of saddles equals to the number of nodes ($\equiv$ roots of $H(\cdot, \cdot, \alpha^* + z) = 0$). Further numerical experiments have confirmed that the flow patterns of $\psi^{*r}(\cdot, t; z)$ do not change qualitatively when varying z in the same regularity region ($|z|$ has to be comparatively small, of course). It complies with Conjecture 2.14 again.

Fig. 5.4 demonstrates the significance of the flow $\psi(\cdot, t; z)$ for the convergence of a discrete version of Newton method. We have in mind the iterations (3.6), replacing naturally $\mathscr{M}$ by the vector field $\mathscr{M}^*$ that is related to our particular germ h. We consider the variant without a damping (i.e., $d = 1$). Let $z = (-0.01, -1)$ be the same as the imperfection selected for the experiment on Fig. 5.3. Fig. 5.4 shows the computed basins of attraction $\mathfrak{B}^1_{\mathscr{M}^*}((x_j, s_j); z)$, $j = 1, 2, 3$, of the three nodes (x_j, s_j) of $\psi(\cdot, t; z)$ from Fig. 5.3. These attractors are marked by circles on Fig. 5.4. The relevant basins are shadowed in black and two tones of grey. As far as the correspondence between a particular attractor and the colour of its basin is concerned, mind the local covergence property of Newton iterations. The significance of the saddles from Fig. 5.3 becomes apparent when these are projected into Fig. 5.4: At these points, boundaries of several basins cross each other. (It motivates the label "cross point" from Definition 4.6).

One may recognize another two "cross points" of black with dark grey, and dark grey with light grey basins. These have no counterpart on Fig. 5.3. Taking a larger window in the (x, s)-plane, we would register a lot of cross points of that kind. They

can be characterised as pre-images of the three saddles on the critical set (i.e., the iteration (3.6) take them, after several steps, in one of the mentioned saddles on the critical set).

The analogous experiment with Newton iterations for the same imperfection $z = (0.1, 0)$ as on Fig. 5.2, is not reported here. There is (naturally) just one basin of attraction that covers the whole window in the (x, s)-plane that is considered on Fig. 5.2. Nevertheless, the saddle point from Fig. 5.2 plays a role of a troublemaker. It may divert (for a while) the iterations from the direction towards the attractor.

The Conjecture 3.6 was tested on the same example of $F\colon \mathbb{R}^4 \times \mathbb{R}^1 \times \mathbb{R}^2 \to \mathbb{R}^4$ that was considered in [5]. The mapping F can be related to a steady-state 3-box Brusselator model (we refer e.g. to [15] for a detailed description of this class of reaction-diffusion problems). We define

$$F(u, \lambda, \alpha) = \begin{cases} D\left(w^{(2)} - w^{(1)}\right) + \lambda f\left(w^{(1)}\right) + \varepsilon E w^{(1)} \\ 2D\left(w^{(1)} - w^{(2)}\right) + \lambda f\left(w^{(2)}\right) + 2\varepsilon E w^{(2)} \end{cases} \tag{5.1}$$

where $u = (u_1, u_2, u_3, u_4)^\mathsf{T} \in \mathbb{R}^4$, $\lambda \in \mathbb{R}^1$, and $w^{(i)}$ are auxiliary vectors that are related to u such that $w^{(1)} = (u_1, u_2)^\mathsf{T}$, $w^{(2)} = (u_3, u_4)^\mathsf{T}$. The operator depends on a number of unfolding parameters namely, D and E are 2×2 diagonal matrices and

$$f(w) \equiv \begin{pmatrix} A - (B+1)w_1 + w_1^2 w_2 \\ B w_1 - w_1^2 w_2 \end{pmatrix} \quad \text{for} \quad w = (w_1, w_2)^\mathsf{T} \in \mathbb{R}^2.$$

In order to have just two imperfection parameters, we fix $D = \mathrm{diag}(1, 10)$, $E = \mathrm{diag}(1, 1)$ and $A = 2$. The parameters ε and B are set free. Thus, $\alpha = (\varepsilon, B) \in \mathbb{R}^2$.

The point $(u^*, \lambda^*, \alpha^*) \in \mathbb{R}^4 \times \mathbb{R}^1 \times \mathbb{R}^2$,

$$u^* = (2,\ 1.425,\ 2,\ 1.425),\ \lambda^* = 8.095771,\ \alpha^* = (0,\ 2.85) \tag{5.2}$$

serves as an example of a pitchfork bifurcation points that meets all requirements of this Section. The choice

$$L = (0, -1, 0, 1) \quad , \quad M = \tfrac{1}{2}(-1, 1, 1, -1)^\mathsf{T}$$

of bordering vectors guarantees that $(u^*, \lambda^*, \alpha^*) \in \mathfrak{D}$.

The imperfection $z = (-10^{-6}, 0)$ belongs to the regularity region that yields three regular roots of the extended system $H(u, \lambda, \alpha^* + z) = 0 \in \mathbb{R}^5$ for turning points $(u, \lambda) \in \mathbb{R}^4 \times \mathbb{R}^1$. The phase portrait of the resulting (reduced, and regularised) Newton flow $\psi^r(\cdot, t; z)$ is depicted on Fig. 5.5. The window in the (x, s)-plane contains all expected fixed points of the flow. The flows on Fig. 5.3 and Fig. 5.5 are clearly topologically equivalent. This observation complies with Conjecture 3.6.

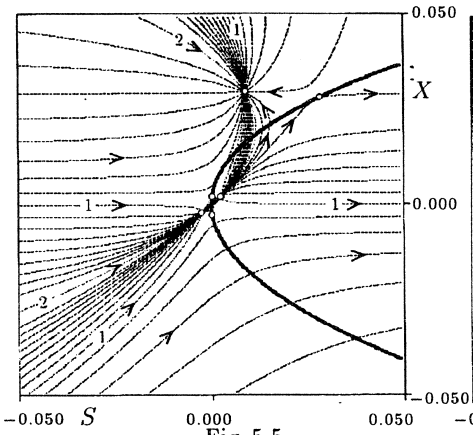

Fig. 5.5

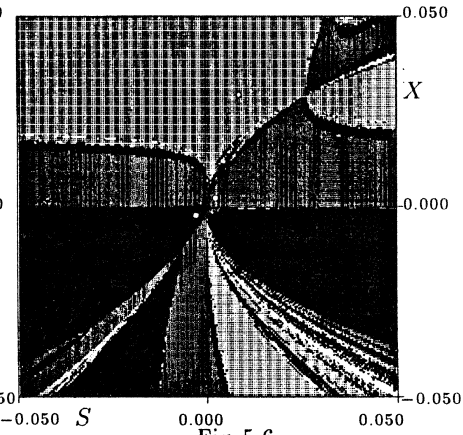

Fig. 5.6

Remark 5.1. A number of numerical experiments that could not be reported here, confirm the strong belief that Conjecture 3.6 might be true when the flow ψ^r is organized by a pitchfork bifurcation singularity. In other words, the flow patterns on Figs.5.1–3 might be significant for $\psi^r(\cdot, t; z)$ under an arbitrary sufficiently small perturbation z, provided that ψ^r is related to a pitchfork bifurcation point $(u^*, \lambda^*, \alpha^*)$. Moreover, the numerical tests comply with Conjecture 2.14: The mentioned flow patterns correspond to particular regularity regions of z. In fact, if the choice of $z \neq 0$ yields locally one root (and three roots) of $H(\cdot, \cdot, \alpha^* + z) = 0$ then the flow pattern of $\psi^r(\cdot, t; z)$ corresponds to that on Fig. 5.2 (and Fig. 5.3, respectively).

Let us report on numerical experiments with classical Newton iterations (1.7). We stick to the above example (5.1–2), and consider the same imperfection $z = (-10^{-6}, 0)$. Fig. 5.6 depicts the basins $\mathfrak{B}^1_{\mathcal{N}}(\cdot; z)$ of attraction (shadowed in black and two tones of grey) for each of the nodal points of $\psi^r(\cdot, t; z)$ from Fig. 5.5. In order to get a planar picture (note that the mentioned basins are subsets of $\mathbf{R}^4 \times \mathbf{R}^1$), we restricted the basins to the invariant manifold $\mathfrak{I}(z)$ from Theorem 3.1. As it was noted in §3, this manifold is not invariant for the discrete dynamical system (1.7). In our experiment, $\mathfrak{I}(z)$ serves just as a set of initial conditions for the iterations (1.7). We have used (x, s) as natural coordinates on $\mathfrak{I}(z)$. Projecting the saddle points from Fig. 5.5 into Fig. 5.6 (note that both refer to the same window in $\mathbf{R}^2$), one will immediatelly understand the significance of these saddles as "cross points" of various basins of attraction. In principle, Fig. 5.6 exhibits similar qualitative features as Fig. 5.4. Fig. 5.8 reports on the same experiment as Fig. 5.6, collecting the data on a substantionally larger window in $\mathfrak{I}(z)$.

In (ω, x, s, z)-coordinates that were introduced for the purpose of Central Manifold Theorem (Theorem 3.4), we may refer to $\mathfrak{I}(z)$ as to the set

$$(5.3) \qquad \{(\omega, x, s, z) \in \operatorname{Im} Q \times \mathbb{R}^1 \times \mathbb{R}^1 \times \mathbb{R}^2 \colon w \equiv Q\, y,\ y \in \mathbb{R}^4,\ z \equiv (-10^{-6}, 0)\},$$

fixing $y = 0$. Obviously, the basins $\mathfrak{B}^1_{\mathcal{N}}(\cdot; z)$ can be restricted to any of the 2-dimensional manifolds from the family (5.3). The particular manifold is selected by a choice of $y \in \mathbb{R}^4$.

Fig. 5.7 and Fig. 5.9 depict such a restriction to the manifold that is characterised by the choice $y \equiv (0, 0.1, 0, 0)$. Note that the selected windows in the (x, s)-plane correspond to the windows on Fig. 5.6 and Fig. 5.8. The significant difference between Fig. 5.6 and Fig. 5.7 (and, similarly, between Fig. 5.8 and Fig. 5.9) seems to be just a shift in s-direction. Conjecture 3.5 claims in fact that various slices (characterised by a fixed choice of y) of the basins $\mathfrak{B}^1_{\mathcal{N}}(\cdot; z)$ should be qualitatively the same (at least when $\|y\|$ is small). The results of the reported experiment comply with the claim.

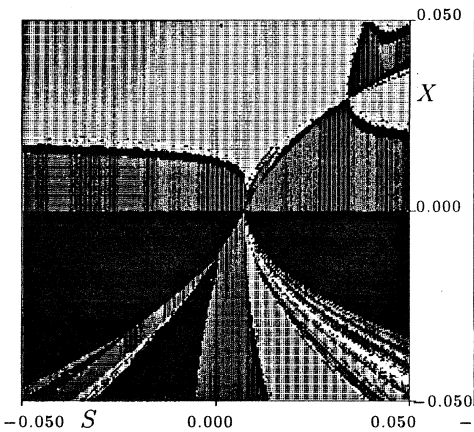

Fig. 5.7

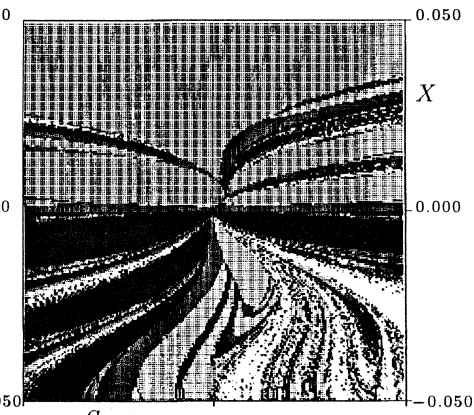

Fig. 5.8

The same conclusion was made for a number of level sets (5.3) characterised by a choice of y that would not exceed the upper bound $\|y\| < 0.1$. Mind you that the imperfection z that has been considered, is really very tiny. Taking z slightly larger in modulus, the size of the windows has to be changed dramatically in order to get "nice" pictures.

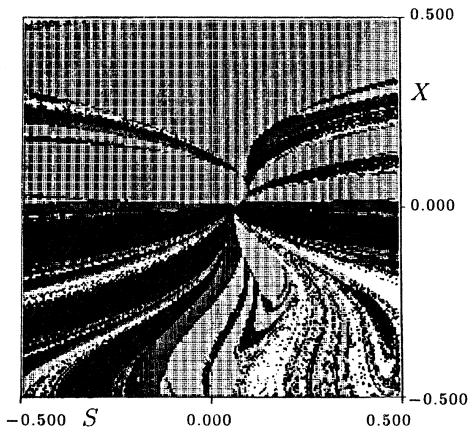

Fig. 5.9

6. A CASE STUDY: ASYMMETRIC CUSP

The aim is to report on some numerical experiments with Newton method (1.7) and (1.8) assuming that the Newton field (1.5) is "organized" by an *assymmetric cusp*, see Definition 2.9.

As a model problem, we consider the unfolding $h(x, s, z) = x^2 + s^3 + z_1 + z_2 s$ of the relevant normal form (see Table 2.12). There are just two regularity regions related to h, see the regions marked as 2 and 4 on Fig. 6.1. The mapping $h(\cdot, \cdot, z)$: $\mathbf{R}^1 \times \mathbf{R}^1 \to \mathbf{R}^1$ has one turning point (and three turning points) when z is chosen from the region 2 (and region 4, respectively). These turning points are fixed points (nodes) of vector field $\mathcal{M}^*(\cdot, z)$, see (3.10). If z is on a transition set (these are marked as 3 and 5) then there are just two turning points. One of them always degenerates into either a *simple bifurcation point* or an *isola formation centre*. The former case happens if z belongs to the set 3, the latter case take place when z is from the transition set 5. If $z = 0$ then there is just one turning point that degenerates into the point classified as *asymmetric cusp*.

We may look at the turning points as (regular, or singular) roots of the mapping $H(\cdot, \cdot, z)\colon \mathbf{R}^2 \to \mathbf{R}^2$, $H(\cdot, \cdot, z) \equiv (h(\cdot, \cdot, z), h_x(\cdot, \cdot, z))^\mathsf{T}$ that is defined in a clear analogy with (1.1). As it was mentioned, we may also interprete the ("nondegenerate") turning points as fixed points of $\mathcal{M}^*(\cdot, z)$. Let $\mathcal{M}^{*r}(\cdot, z)$ denote the regularised version of $\mathcal{M}^*$, see (3.14). The turning points that are available in the above scenario can be also understood as (hyperbolic, or nonhyperbolic) fixed points of $\mathcal{M}^{*r}(\cdot, z)$ on $\mathbf{R}^2$. We already know that there are fixed points of $\mathcal{M}^{*r}(\cdot, z)$ (located necessarily on $\mathfrak{C}_{\mathcal{M}^*}(z)$) that could not be interpreted as roots of $H(\cdot, \cdot, z) = 0$. We used to

call them cross points. These have an important influence on the performace of any variant of Newton method.

We start with the analysis of the flow $\psi^{*r}(\cdot, t; z)$ that is defined by $\mathcal{M}^{*r}(\cdot, z)$ on $\mathbf{R}^2$. In accordance with Conjecture 2.14, we would expect just one flow pattern provided that z were ranging in one regularity region. It is true as far as the region 4 on Fig. 6.1 is concerned: The typical phase portrait of $\psi^{*r}(\cdot, t; z)$ is plotted on Fig. 6.3 ($z = (0, -0.2)$). Here and in the forthcoming pictures, the thick verticals represent critical sets $\mathfrak{C}_{\mathcal{M}^*}(z)$.

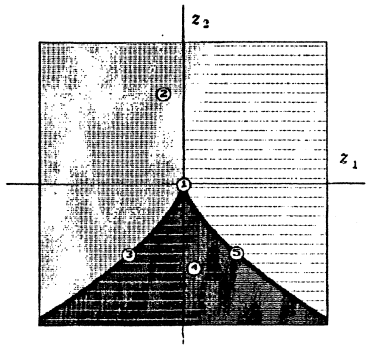

Fig. 6.1

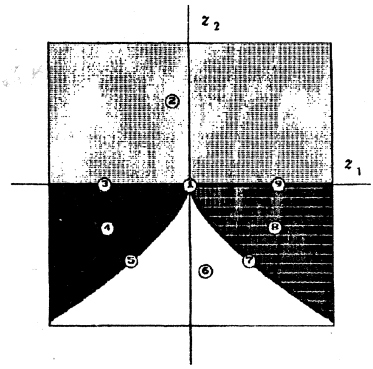

Fig. 6.2

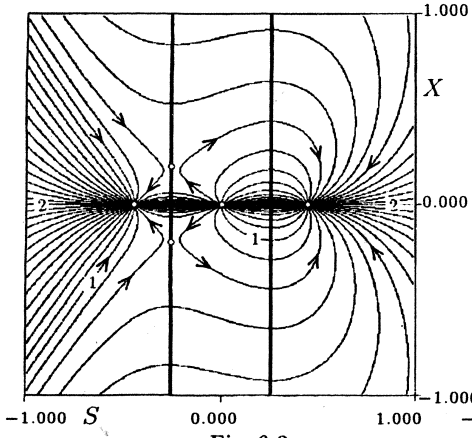

Fig. 6.3

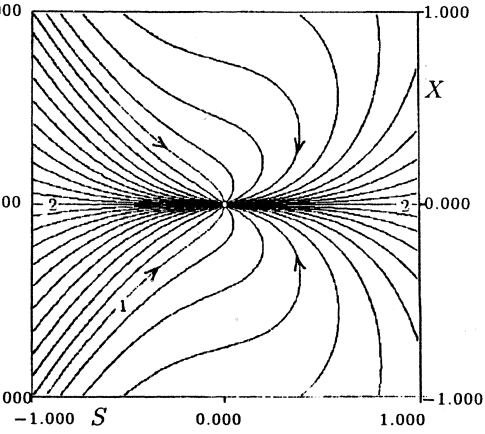

Fig. 6.4

In the regularity region 2 from Fig. 6.1, there could be distinguished three subregions of imperfections z that lead to a qualitatively different behavoir of $\psi^{*r}(\cdot, t; z)$.

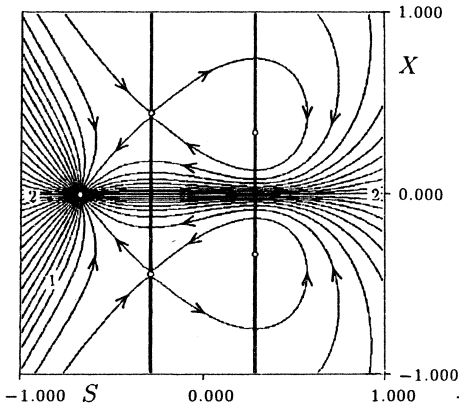

Fig. 6.5

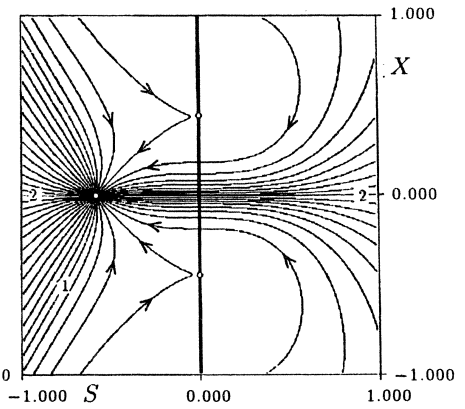

Fig. 6.6

These subregions are related to the subsets that are labeled as 2, 3, 4, 8 and 9 on Fig. 6.2. The relevant flow patterns are sketched on Figs.6.4–6. In particular, Fig. 6.4 is computed for the imperfection $z = (0, 0.2)$. It illustrates the flow when z belongs to the subregions 2, 3 and 4 on Fig. 6.2.

It should be noted that as far as the ("nonregularised") flow $\psi^*(\cdot, t; z)$ is concerned, it can be shown that the critical set is empty when z is taken from the subregion 2. If z belongs to 4 and 3 then there exists the critical set $\mathfrak{C}_{\mathscr{M}^*}(z)$ that consists of two and one straight lines parallel to x-axis, respectively. Consequently, the flow patterns of $\psi^*(\cdot, t; z)$ for z from 2, 3 and 4 are not topologically equivalent.

Fig. 6.5 ($z = (0.149, -0.25)$) and Fig. 6.6 ($z = (0, 0.2)$) illustrate the phase portraits of the flow $\psi^{*r}(\cdot, t; z)$ when z belongs to the subregions 8 and 9, respectively. The transition of the flow $\psi^{*r}(\cdot, t; z)$ as z varies from the region 8 to the region 2 (e.g., the transition of the flow on Fig. 6.5 to the flow on Fig. 6.4) is organized by two nonhyperbolic fixed points on $\mathfrak{C}_{\mathscr{M}^*}(z)$ when z happens to be on the set 9, see Fig. 6.6 for an example. Note that the relevant flow is locally Hamiltonian (see Remark 3.12).

If z is chosen from the transition set labeled as 5 and 7, respectively, the typical flow patterns are depicted on Fig. 6.7 and Fig. 6.8. (Here, the particular z are defined as $z = (2s^3, -3s^2)$ for $s = 0.303$ and $s = -0.303$, respectively.) The nonhyperbolic fixed points of $\mathscr{M}^{*r}(\cdot, z)$ organize the flow $\psi^{*r}(\cdot, t; z + \delta z)$ for small variations of δz. Note that the mentioned organizing centres are a simple bifurcation point and an isola formation centre, respectively. The perturbation of $\psi^{*r}(\cdot, t; z)$ is then well understood (see Theorem 3.7 and Remark 3.8). It explains the transitions from Fig. 6.3 to Fig. 6.4 and from Fig. 6.3 to Fig. 6.5.

The highest degeneracy of the flow is achieved for $z = 0$, see Fig. 6.9 for the relevant phase portrait.

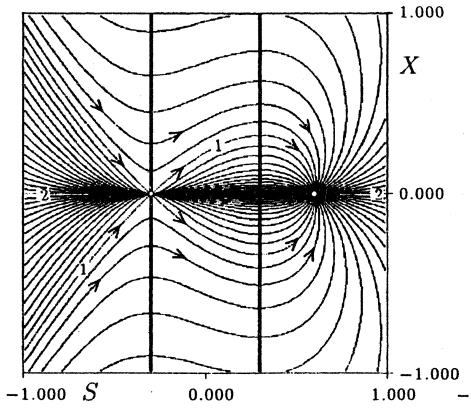

Fig. 6.7

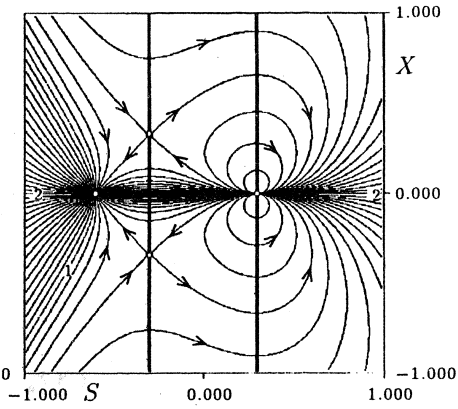

Fig. 6.8

As far as the continuous Newton method is concerned, the above experiment contradicts Conjecture 2.14. On the other hand, the performance of discrete versions of Newton method seems to be in an agreement with that conjecture. Eventhough the flow $\psi^*(\cdot, t; z)$ exhibits qualitatively different flow patterns when z is chosen from the regions 2, 3, 4, 8 and 9 (Fig. 6.2), there exists just one basin of attracion $\mathfrak{B}^d_{\mathcal{M}^*}(\cdot; z)$ of damped Newton iterations that covers all the window in the (x, s)-plane.

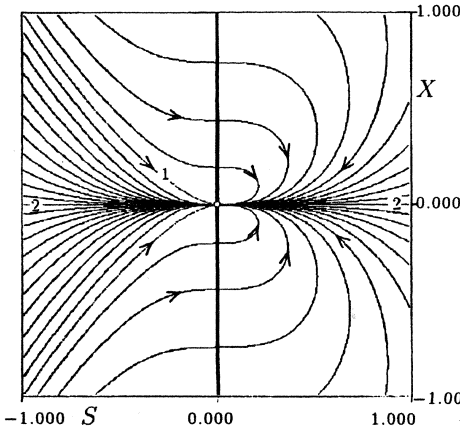

Fig. 6.9

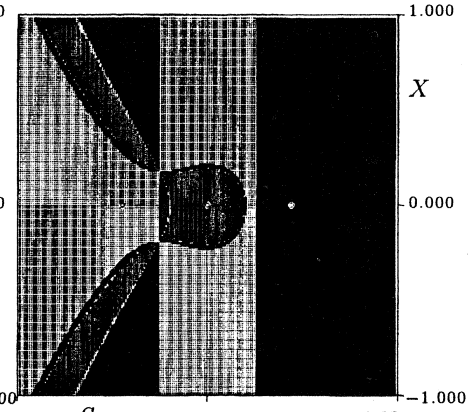

Fig. 6.10

There are naturally three basins of attraction for damped Newton method provided that z belongs to the subset 6. Figs.6.10–12 report on the convergence of damped Newton (with $d = 1$, $d = 0.1$ and $d = 0.01$), assuming the same imperfection $z = (0, -0.2)$ as that on Fig. 6.3. The basins of attraction are shadowed in black and

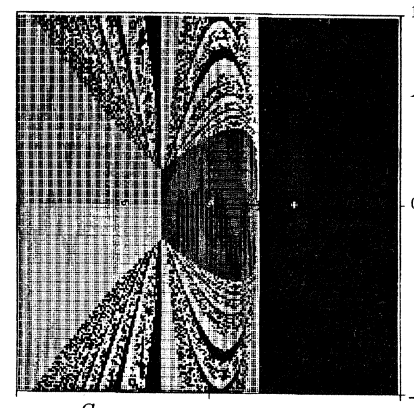

Fig. 6.11

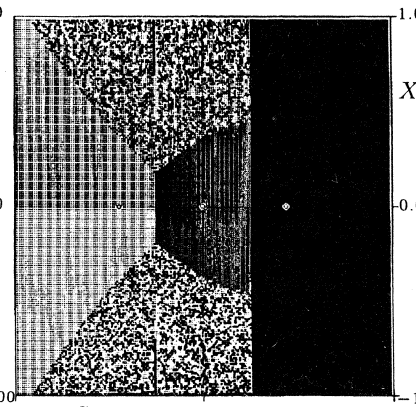

Fig. 6.12

two tones of grey. Again, the saddles from Fig. 6.3 play an important role as "cross points" of the basins of attractions. Due to a heavy damping (Fig. 6.12), discrete Newton iterations seem to take over some qualitative features of the continuous Newton: The "chaotic" region on Fig. 6.12 clearly fits in the region in Fig. 6.3 that is taken by $\psi^*(\cdot, t; z)$ in one of the critical sets (we might call the region as a *divergence region* of the flow $\psi^*(\cdot, t; z)$). The separatrixes of the flow (Fig. 6.3) are, in fact, boundaries of the chaotic region on Fig. 6.12.

References

[1] *Branin F.H.*: A widely convergent method for finding multiple solutions of simultaneous non-linear equations, IBM J. Res. Develop. (1972), 504–522.

[2] *Golubitski M., Schaeffer D.*: Singularities and Groups in Bifurcation Theory Vol. 1, Springer Verlag, New York, 1985.

[3] *Griewank A., Reddien G. W.*: Characterisation and computation of generalised turning points, SIAM J. Numer. Anal. *21* (1984), 176–185.

[4] *Guckenheimer J., Holmes P.*: Nonlinear Oscillations, Dynamical Systems and Bifurcation of Vector Fields, Appl. Math. Sci. 42, Springer Verlag, New York, 1983.

[5] *Janovský V., Seige V.*: Qualitative analysis of Newton iterations for imperfect bifuracation singularities, I. A case study, submitted to SIAM J.Numer.Anal..

[6] *Jepson A.D., Spence A.*: Singular points and their computation, In: Numerical Methods for Bifurcation Problems (Küpper T., Mittelmann H. D., Weber H., eds.), vol. ISNM 70, Birkhäuser Verlag, Basel, 1984, pp. 502–514.

[7] *Jepson A.D., Spence A.*: A reduction process for nonlinear equations, SIAM J. Math. Anal *20* (1989), 39–56.

[8] *Jongen H.Th., Jonker P., Twilt F.*: A note on Branin's method for finding the critical points of smooth functions, In: Parameteric Optimization and Related Topics (Guddat J., Jongen H.Th., Kummer B., Nožička F., eds.), Akademie Verlag, Berlin, 1987, pp. 196–208.

[9] *Keller H.B.*: Numerical solution of bifurcation and nonlinear eigenvalue problems, In: Applications of Bifurcation Theory (Rabinowitz P.H. ed.), Academic Press, New York, 1977, pp. 359–384.

[10] *Kubíček M., Marek M.*: Evaluation of turning and bifurcation points for algebraic and nonlinear boundary value problems, Appl. Math. Comp. *5* (1979), 106–121.

[11] *Kubíček M., Marek M.*: Computational Methods in Bifurcation Theory and Dissipative Structures., Springer Verlag, New York, 1983.

[12] *Melhem R.G., Rheinbold W.C.*: A comparison of methods for determining turning points of nonlinear equations, Computing *29* (1982), 201–226.

[13] *Peitgen H.O., Prüfer M.*: Global aspects of Newton's method for nonlinear boundary value problems, In: Numerical Methods for Bifurcation Problems (Küpper T., Mittelmann H. D., Weber H., eds.), vol. ISNM 70, Birkhäuser Verlag, Basel, 1984, pp. 352–368.

[14] *Pönisch G., Schwetlick H.*: Computing turning points of curves implicitly defined by nonlinear equations depending on a parameter, Computing *26* (1981), 107–121.

[15] *Raschman R., Schreiber I., Marek M.*: Periodic and aperiodic regimes in linear and cyclic arrays of coupled reaction diffusion cells, In: Lect. in Appl. Math. Vol. 24, pp. 61–100 (1986), AMS, Providence, RI.

[16] *Saupe D.*: Discrete versus continuous Newton's method, Acta Applicandae Mathematicae *13* (1988), 59–80.

[17] *Smale S.*: On the efficiency of algorithms of analysis, Bull. A.M.S. *13* (1985), 87–121.

[18] *Spence A., Werner B.*: Nonsimple turning points and cusps, IMA. J. Numer. Anal. *2* (1982), 413–427.

Authors' address: *Vladimír Janovský, Viktor Seige*, Department of Numerical Analysis, Faculty of Mathematics and Physics, Charles University, Malostranské nám. 25, Prague, Czech Republic.